KWAME NKRUMAH UNIVERSITY OF SCIENCE AND TECHNOLOGY,

KUMASI, GHANA

Performance Evaluation of Spatial Diversity Based Free Space Optical Communication Links over Atmospheric Turbulence Channels

By

Emmanuel Kweku Hinson (BEElectronics and Communication Engineering)

PG5903511

A Thesis submitted to the Department of Electrical/Electronic Engineering,

College of Engineering

In partial fulfillment of the requirements for the degree of

MSc Telecommunication Engineering

JANUARY 2015

Declaration

I hereby declare that this submission is my own work towards MSc Telecommunication Engineering and that, to the best of my knowledge; it contains no material previously published by another person, nor material which has been accepted for the award of any other degree of the University, except where acknowledgement has been made in the text.

Emmanuel K. Hinson (ID: PG5903511)

(Student Name and Index Number)

Signature: …….

Date: …….

Certified by:

Dr. James D. Gadze (Supervisor)

Signature: ……

Date: ……

Prof. P.Y. Okyere(Head of Department)

Signature: …….

Date: …….

Acknowledgements

I will like thank the Almighty God for his love and protection throughout my MSc program. My profound gratitude goes to Dr. J.D. Gadze for his support for this thesis. He provided the guidance and supervision towards making this thesis a success. I will also love to thank Mr. Prince Anokye for his support during this thesis. My appreciation further goes to the entire members of the Department of Electrical/Electronic Engineering for their commitment towards this thesis. Much thanks to my lovely wife for her love and support during those stressful moments of my MSc program.

Abstract

The ever increasing bandwidth demand on wireless communication systems has led to the development of several wireless technologies. Free Space Optical (FSO) Communication promises high speed data transmission, license-free operation, highly secured transmission and immunity to electromagnetic interferences. However index-of-refraction turbulence (IRT) has limited the performance of FSO communication systems by causing fast fluctuations in the received optical intensity and increasing the Bit-Error Rate (BER). As a result, several mitigation techniques have been proposed to reduce the effects of turbulence. This thesis evaluates the BER performance of spatial diversity based FSO links. We have characterized IRT using the PDF of gamma-gamma distribution. The Scintillation index (SI), statistical measure of IRT, has been shown to depend on the gamma-gamma parameters. Lower values of GG parameters lead to higher SI and therefore increasing IRT along the propagation path and average BER. We have derived closed-form expressions for the average BER by employing multiple receive and/or transmit apertures. Numerical results show significant reduction in the average BER as the number of transmit apertures or receive apertures are increased. Thus, offering substantial improvement in the performance of FSO links over IRT channels.

Table of Contents

List of Figures

Chapter One

Introduction

1.1 Background and Motivation

Over the past years, wireless communications technologies have been comprehensively researched in order to exploit the beneficial properties they have over wired communication technologies. These advantages include mobility and flexibility. Several wireless communication devices are being developed at an exponential growth rate. Today, traditional voice communication is not the only demand on these wireless devices. Many bandwidth demanding multimedia applications are being run on these devices putting serious strain on wireless communication systems. In response to the ever increasing bandwidth demand, several wireless communication technologies are being developed. The problem is to developmore scalable and adaptive networkscapable of supporting the demand for high speed data. WiMax and Millimeter Wave and Free Space Optical (FSO) communication technologies have been proposed by researchers for next generation networks.In comparison to these alternatives, FSO is more attractive due to its potential to provide high data rates.

Free Space Optical (FSO) Communication is the transmission of high speed data using optical signals propagating through the atmosphere (i.e. free space). Due to its wide range of applications [1], [2], FSO can be considered as a workable technology for next generation networks.Links involving satellites, deep-space probes,ground stations, unmanned aerial vehicles (UAVs), high altitude platforms (HAPs) and aircrafts are some of the practical

applications of FSO communication [3]. Further, both military and civilian applications can employ FSO communication.

The advantages of FSO communication comes from the properties of optical signals. Firstly, FSO can provide high data rates in the gigabits/sec range. Secondly, it does not require licensing for its operation. This is because the electromagnetic band occupied by optical signals does not require licensing from local authorities. This is a major cost advantage over other wireless technologies (i.e. microwave). Furthermore, FSO communication has very high immunity against electromagnetic interference (EMI) and promises highly secured transmission. This is due to the low probability of interception and low probability of detection (LPI/LPD) properties of optical signals [4]. Due to the high data rates associated with FSO communication, the last mile connectivity problem can be solved.

However, the FSO communication'sreliability is highly susceptible to changes in the conditions of the atmosphere. Optical signals propagating through the atmosphere suffer from Index-of-Refractive Turbulence (IRT). Turbulence-induced[1] fading impacts negatively on the FSO transmissions particularly for propagation paths of 1 kilometer or more [2]. Turbulenceinduced fading is the fast fluctuations of the received intensity occurring as a result of random variations of the refractive index.Temperature and pressure inhomogeneity of the atmosphere causes variations in the refractive index leading to deterioration in the received image quality. This can cause the intensity and phase of the optical signal to fluctuate rapidly [5]. This rapid fluctuation in the received optical signal is also called scintillations. Scintillations increase error probability of FSO link, reducing FSO communication systemsperformance. Several statistical distributions have been suggested to study turbulence

[1] Fast fluctuations of the received signal intensity occurring as a result of random variations of the refractive index of the atmosphere.

in optical signals propagating through the atmosphere [2]. Scattering effects caused by molecular and aerosol particles of the atmosphere also reduce the performance of FSO communication systems [6], [7], but are not the subject of this research.Again misalignment between the transmitter and receiver [1]caused by building sway can lead to loss in link performance. Misalignment effect is also not considered.

Turbulence-induced fading significantly reduces the reliability of the optical link and increases the error rate. Powerful mitigation techniques are therefore needed to decrease the impact of atmospheric turbulence. Two major techniques have been proposed in literature to mitigate the deleterious impacts of atmospheric turbulence. These techniques are Maximum Likelihood Sequence Detection (MLSD) [5], [8] and Error Control Coding with interleaving [9], [10]. Both techniques however have some practical limitations.MLSD suffers from high computational complexity whilst the Error Control Coding requires large-size interleavers.

Spatial Diversity, a popular mitigation technique in Radio Frequency (RF) communication systems has the potential to provide solution for turbulence-induced fading. By employing multiple receivers and/or the transmitters, Spatial Diversity has the potential to provide improvement of the FSO link performance. This is due to the inherent redundancy associated with the system arrangement. Optical beams blockage by obstructions such as flying birds and aircrafts can be significantly decreased.Longer distances can also be covered by the transmitted laser beam propagating through thick weather conditions.

1.2 Research Motivation

The emergence and explosion of mobile smart devices in Ghana is the main motivation behind this research. The bandwidth demand on communication systems in Ghana is increasing at an

exponential rate. To meetthis bandwidth demand, telecommunication companies are investing huge capital in fiber optic communication systems for their backbone networks. Installation of fiber optic cables involves digging and burying cables which require licensing from local authorities (e.g. KMA and AMA). Some of these cables are destroyed during road constructions. In highly populated areas, it is difficult if not impossible to install fiber optic cables. Telecommunication companies are therefore forced to depend on microwave links for their backbone network. FSO communication can be used as an alternative or a backup to provide the backbone network. Again, small and medium scale companies require high speed data transmission but are deterred by the high cost involved in fiber optic systems. FSO can offer more cost effective and high data rates as an alternative. The last mile connectivity issues associated with microwave can be solved by using FSO communication.

1.3 Problem Statement

Free Space Optical (FSO) communication has the potential to provide cost effective, high speed data, license-free operation and highly secured transmissions. However, turbulenceinduced fading significantly impairs the performance of the FSO link by increasing the error rate and reducing the link's reliability. It is therefore imperative to seek effective mitigation techniques to combat turbulence-induced fading. This thesis seeks to evaluate the performance of Spatial Diversity based FSO links.

1.4 General objective

The main objective of this thesis is to study and analyze the performance of Spatial Diversity to mitigate the effects of turbulence-induced fading in FSO communication systems.

1.4.1 Specific Objectives

The specific objectives of this study are:

1. To model turbulence-induced FSO channel using statistical distribution.
2. To evaluate the Bit-Error-Rate (BER) of a Single-Input Single-Output (SISO) FSO link over Index-of-Refraction Turbulent (IRT) channel as a benchmark.
3. To derive accurate closed-form expression for the BER of multiple apertures at the receiver and/or transmitter.

1.5 Thesis Organization

The rest of this thesis is organized as follows: Chapter 2 presents review of existing literature on turbulence mitigation techniques. Chapter 3 discusses the system model for spatial diversity mitigation technique. Chapter 4 discusses results of the research and the thesis ends with chapter 5 providing the conclusion and recommendations for future research.

Chapter Two

Literature Review

2.1 Introduction

This chapter presents an overview of Free Space Optical (FSO) Communication. Effects of turbulence-induced fading on FSO communication systems are discussed with the view of deepening understanding. Mitigation techniques in literature are reviewed with the aim of identifying research gaps.

2.2 Overview of Free Space Optical Communication

Free Space Optical Communication is the transmission of data using optical signals propagating through the atmosphere. The data to be transmitted can be modulated in the intensity, frequency or phase. FSO is essentially a line-of-sight (LOS) communication technology. Thus to ensure successful data exchange requires the establishment of a clear LOS propagation path between the transceiverswithout any form of obstruction in their path. Figure 2.1 shows the basic setup of FSO. Transmitted laser beams have narrow beam widths and divergence of few *mrads* and receivers have small angle field of view.Typical laser beams employed in FSO communication have diffraction limited divergence angle between 0.01mrad – 0.10mrad [11].

Figure 2.1 Basic FSO Communication Setup [12]

FSO communication has more advantages over other wireless communication technologies. Firstly, it can provide high data rates (i.e. Gigabits data). The information carrying capacity of every communication system is proportional to the bandwidth of the carrier signal; which is also proportional to the carrier frequency. On the electromagnetic spectrum, optical signals have the highest possible frequency (i.e. frequency range of 20THz - 375THz) of practical interest in communication. Optical signals therefore promise the highest possible theoretical data rates. FSO communication can provide higher data rates than microwave communication systems. Microwave systems have the highest data rates among wireless technologies so far.

Moreover, FSO communication promises highly secured transmission with low probability of interception/ low probability of detection (LPI/LPD) properties [4]. This is due to the narrow beam width and small divergence angle of laser beams. Unlike microwave signals, transmitted optical signals cannot be captured by spectrum analyzers or RF meters for analysis [13].

Furthermore, optical signals employed in FSO communication are highly immune to electromagnetic interference (EMI) and therefore provide opportunity for unlimited frequency

reuse. Again, this is due to the narrow beam width and small divergence angle of optical signals employed in FSO communication systems.

Lastly, FSO communication does not require licensing from local regulatory agencies (e.g. National Communications Authority) for its operation. This is a major cost advantage over microwave links. The electromagnetic band occupied by light does not require licensing for operation.

However, FSO communication is highly susceptible to atmospheric conditions (see figure 2.2). Thus the reliability of the communication technology depends largely on atmospheric conditions. Optical signals propagating through the atmosphere suffer from index-ofrefraction turbulence (IRT), scattering and absorption by molecular and aerosol particles of the atmosphere. IRT is the subject of this work and will be discussed in detail. IRT can severely deteriorate the FSO links performance especiallyfor distances greater than 1Km.

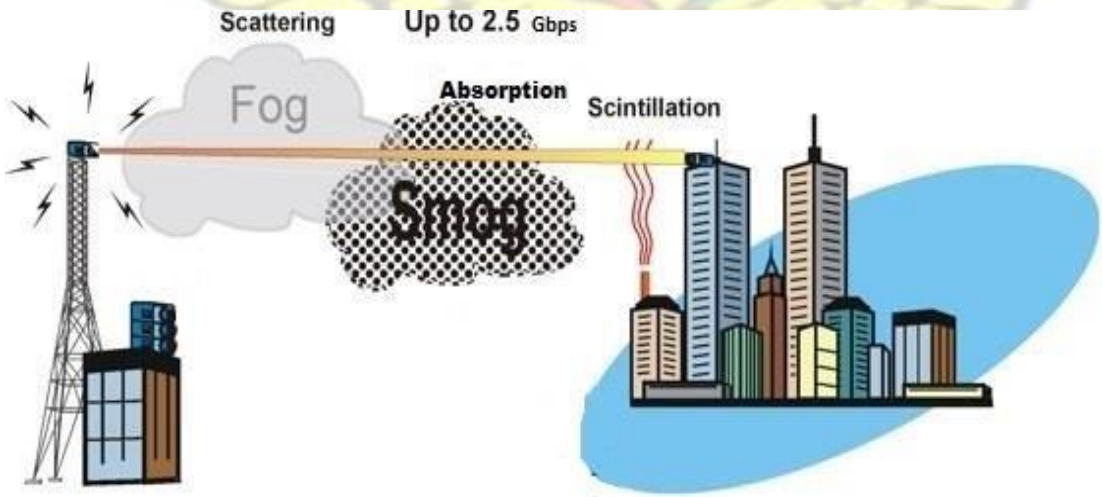

Figure 2.2 Atmospheric Conditions affecting FSO Communication [12]

2.3 Atmospheric Turbulence

When the Earth is struck by solar radiation, the Earth's surface absorbs some of the solar radiation. This leads to the heating up of the surface air mass of the Earth. The surrounding cooler air mass mixes turbulently with the rising warm air mass. This culminates in small (temperature ranges of 0.01 to 0.1 degrees) but spatially and temporally fluctuating atmospheric temperature [11]. The temperature inhomogeneity of the atmosphere causes corresponding variations in the index of refraction of the atmosphere. The varying indices of refractionresult in the formation of eddies. Eddies are cells or packets of air with varying sizes ranging from ~0.1cm to ~10m [14].These eddies act like refractive prisms with changing refractive indices. The propagating light wave is therefore deviated partially or completely depending on the relative size of the beam and the degree of temperature inhomogeneity along the propagation path [11]. Figure 2.3 shows this phenomenon. The changing refractive index of the atmosphere is called Index-of-Refractive Turbulence (IRT).

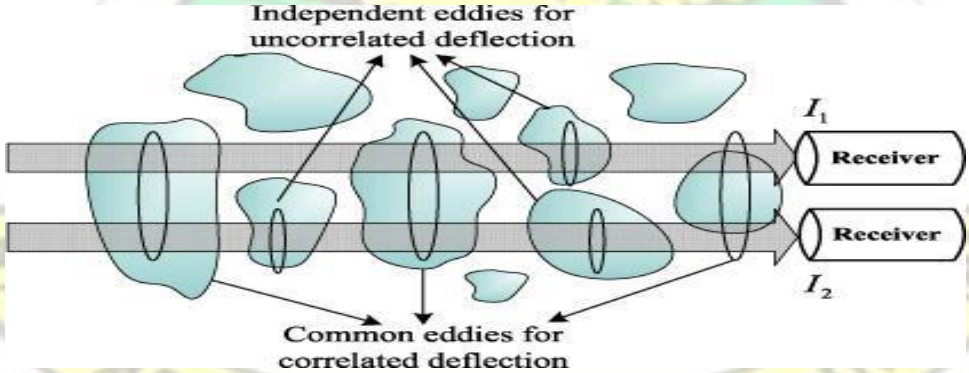

Figure 2.3Illustration of Eddies deflecting optical signals [15]

Wavefront distortions occur as a result of random changes in index of refraction of the earth's atmosphere. Thus if light signalstravel through atmospheric turbulence, redistribution of the

intensity (irradiance) of the original light beam profile occur.Thestructure of the index of refraction along the propagation path is dependent on timebecause of the turbulent mixing of index of refraction cells. As a result thespatial intensity distribution at the receiver plane varies. Consequently, light wave traversing the turbulent atmospheric channel fluctuates rapidly in its phaseandintensity.Some of the effects of atmospheric turbulence known in literature include [16]:

a) *Beam Steering*: Angular deviation of the beam from its original LOS trajectory leading to the transmitted light beam missing the receiver aperture.
b) *Beam Spreading*: The beam divergence increases due to scattering of the beam by eddies resulting in a decrease in the power density of the received optical beam.
c) *Degradation in Spatial Coherence*: Atmospheric turbulence also causes distortions in phase coherence across the beam phase fronts. Phase distortions particularly affect systems employing coherent receivers [17].

The intensity scintillation index,σ_I^2,is employedto measure the strength of scintillations.

Scintillation index is the normalized variance of the beam intensity [2]. It is an analytical measure of the integrated amount of IRT along the channel.

IRT significantly causes negative effects on optical transmission through the atmosphere. It increases the FSO link's outage probability[2] and deteriorates the Bit-Error-Rate (BER) [18, 19]. In view of these, several strategieshave been recommended by researchers to combat the negative effects of IRT. Any mitigation technique must aim at reducing the outage probability or BER or both. In the next section, literature on some of these mitigation techniques will be reviewed whilst identifying research concerns.

[2] The outage probability is the percentage of time during which the optical link is not operational.

2.4 Existing Research Work

Several mitigation strategies have been recommended in literature to enhance the performance of FSO. Some of these strategies include Error Control coding in conjunction with interleaving, Rate Adaptive Modulation schemes, Multihop FSO and Maximum Likelihood Sequence Detection (MLSD).

2.4.1 Error Control Coding in Conjunction with Interleaving

M. Uysal, J. Li and Navidpourin [9] use error control coding methods to combat fading under strong turbulence regime. The authors derive an upper bound on the Pairwise Error Probability(PEP). In conjunction with union-bound technique, the derived PEP is then employedto attain BER. The K-distributionis used to model the strong turbulence conditions. Using K-distribution model, intensity of the optical signal, *I*, is modeled as the product of two independent random variables:

$$I = yz \quad \textbf{(1)}$$

$$\text{Where } f(y) = \exp(-y), \quad y \geq 0 \quad \textbf{(2)}$$

$$\text{And } f(z) = \frac{\alpha^{\alpha} z^{\alpha-1} \exp(-\alpha z)}{\Gamma(\alpha)}, z \geq 0 \quad \textbf{(3)}$$

Where α: parameter describing the effective number of scatters; Γ(.): well-known gamma function; y and z: intensities resulting from small-scale and large-scale eddies respectively. Intensity Modulation/Direct Detection (IM/DD) with On-Off Keying (OOK) is assumed. Convolutional code with code rate of 1/3 and minimum hamming distance of 6 is applied

to obtain the PEPupper bound. The authorsshowBER simulation results upto 10^{-7}but this does not meet the BERtarget for wireless systems.

In [10], J.M. Kahn and X. Zhu employ error control codes to reduce fading due to IRT assuming coded On-Off Keying and weak atmospheric turbulence under joint lognormal distribution. The authors derive an upper bound on the pairwise codeword-error probability expressed as:

$$P_{block} \leq \sum_{j} P(C_j) \sum_{k,C_k \in S_c} P_e(C_j, C_k) \quad \textbf{(4)}$$

Where S_c is the set of all codewords and $P(C_j)$ is the probability that codewordC_j is transmitted. The pairwise error probability (PEP), $Pe(C_j, C_k)$ is the probability that when codewordC_j is transmitted the decoder favors the selection of $C_k$over C_j. This approximate upper bound was then applied to convolutional codes, block codes and turbo codes to obtain the upper bound to their bit-error rate. For further gain inthe performance of bit-error rate, the authors employ large-size interleavers. The drawback of this work is that the approximate upper bound is invalid when applied to strong turbulence regimes. Again, the system requires the use of large-size interleavers which is a practical limitation of the system.

Error control codes provide someperformance improvement in turbulent channels. However, the proposed approaches have practical limitations as they require large-size interleavers to realize the potential coding gains offered theoretically or are invalid when applied to different regimes of turbulence.

2.4.2 Rate Adaptive Transmission

Another mitigation technique proposed in literature is rate adaptive transmission; a popular fading mitigation technique used in RF communication [21, 22]. Adaptive transmission exploits the time-varying characteristics of IRT, permitting transmission of higher data rates in satisfactory turbulence regimes. This is achieved by varying basic transmission parameters (e.g. optical power, modulation order) according to the fading intensity of the channel.

In [23], adaptive transmission schemeusing Sub-carrier Phase Shift Keying (S-PSK) is proposed. The technique is implemented by modifying order of modulation of S-PSK in accordancewith the instantaneous fading state and a predefined requirement for Bit-ErrorRate. Here, the authors show that the adaptive transmission presents substantialgains in terms of spectral efficiency compared to the non-adaptive modulation in moderate-to-strong regimes of turbulence. However in low turbulence regimes, it was less beneficial to do adaptation grounded on instantaneous fading state. The proposed technique is only effective at moderate-to-strong turbulence regimes. Again the predefined BER requirement of 10^{-2} and 10^{-3} far exceed the desired BER of 10^{-9}required of wireless systems.

In [24], the authors consider the use of adaptive symbol rate and transmit-power method under the assumption of an ideal decoder that corrects all errors given that the SNRreceived surpasses a specified threshold. Lognormal fading channelis further assumed. The link varies the symbol period, T, over a finite set of values and the transmit-power depending on the channel state until the received SNR exceeds the given threshold. As the transmit power increases, the BER falls to near-zero and the throughput increases. The authors show that substantial improvement

in the throughput is achieved through both power adaptation and symbol rate adaptation. The weakness in this method is the assumption of an ideal decoder.

This is impractical and may be misleading when applied to real systems.

Rate-adaptive transmission scheme for FSO links over turbulent channels is studied in [25]. The proposed technique jointly uses repetition coding and variable silence periods; taking advantage of the potential time-diversity order (TDO) present in IRT channels. Negative exponential and gamma-gamma fading channels are assumed. Repetition coding is first employed in order to adapt the rate of transmission to the channel conditions until the entire TDO present in the IRT channel is completely exploitedby interleaving.The peak-to-average optical power ratio (PAOPR) (High PAOPR have been proven to be a satisfactory characteristic in FSO systems employing IM/DD [26, 27, 28]) is increased by using the variable silence periods. The authors show an increase in the PAOPR hence an improved performance over non-adaptive systems. A target BER of 10^{-8} is achieved at a received SNR of 150dB at a capacity of 1bit per channel. By reducing the capacity to 0.5bit per channel, the same BER of 10^{-8} is attained at 74dB received SNR. The drawback of this method is the low capacity achieved. Again the target BER of $10^{-8}$is achieved at very high SNR.

Authors in [29] propose an adaptive modulation scheme operating through atmosphericturbulence using S-PSK. S-PSK modulation order is alteredin accordance with the instantaneous turbulence and predefined BER. Thespectral efficiency and the average BER performance metrics are evaluated under diverse turbulent regimes. It is shown that by adapting the modulation order the spectral efficiency is significantly improved compared to non-adaptive techniques. The weakness of this method is that it is more efficient to do adaptation

based on the average SNR instead of the instantaneous fading state. Again, achieved average BER exceeds the BER requirements of wireless systems.

Rate-adaptive transmission offers significant improvement in the spectral efficiency, capacity and average BER. However the technique is based on the assumption of a perfect knowledge of CSI which is very difficult to achieve in practical systems. For practical implementations, pilot symbol assisted receiver structures [30] are needed; leading to redundant overhead transmissions and increasing the complication of the implementation (need for data framing and packetization [31]).

2.4.3 Maximum Likelihood Sequence Detection (MLSD)

Mitigation techniques can be used to combat turbulence-induced irradiance fluctuations in regimes in where the receiver diameterD_o, is lesser than the correlation lengthof fading, $d_o$and the observation time T_o, is lesser thanthe correlation timeof fading, τ_o (i.e. $D_o<d_o$ and $T_o<\tau_o$). Maximum likelihood sequence detection (MLSD) techniques exploit knowledge of these two important parameters (i.e. fading correlation length and fading correlation time) of atmospheric turbulence. If the receiver knows the joint temporal statistics of the fading, MLSD can be used.To use MLSD, multidimensional integration is needed and its computational complexity growswith the length of the sequence of bits sent. To detect *n*-bit sequence requires a complexityof $n\square 2^n$. This is because it requires an n-dimensional integration for each of the 2^n sequence of bits.

ML detection scheme is employed in [5], based on the statistical distribution of fading induced by turbulence. If there is no knowledge of the instantaneous fading state but there is knowledge of the marginal fading statistics, ML symbol-by-symbol detection is used to enhancethe

efficiency of detection. If there is knowledge of the temporal correlation of fading, MLSD is employed to offer additional detection performance. However the proposed technique is computationally complex making it impractical for most applications.

X. Zhu*et al* in [32] extended their results in [5] and proposed an optimal MLSD assuming IM/DD. A single-step Markov Chain (SMC) model is proposed to simplify MLSD. The SMC model is applied to achieve an approximate higher order bit errors distribution as well as two reduced-complexity MLSD algorithms based on suboptimal per-survivor processing (PSP). The idea behind PSP is to apply the received intensity of the recently detected *ON* bits to decrease the uncertainty about the turbulence-induced fadingcondition. The authors further argue that if AWGN is considered and the SMC model for the fading temporal correlation is applied then knowledge of the correlation between two consecutive *ON* bits is enough to employ MLSD. This suboptimal approach requires complexity of n^2. The simulation results show significant improvement in the bit-error probability performance over symbol-bysymbol detection. However the proposed technique is still computationally intensive for most practical applications.

In [33], a blind detection technique for OOK FSO systems described by the general Poisson photon-counting detection model is proposed. Based on the generalized maximum likelihood sequence estimation (GMLSE) principle; a sequence detection rule which sufficiently takes advantage of the temporal behaviors of turbulence is used. By applying only the observed received sequence values, the proposed decision rule avoids computation of complex decision metrics.Knowledge of CSIis not required. The authors show significant performance close to the systems employing the optimal MLSD and knowledge of CSI. However simulation results show that the suggested receiver structure performs badly.

MLSD mitigation techniques are quite computationally complex as they require

multidimensional integration making them unattractive for most practical applications.

2.4.4 Multihop Free Space Optics

Multihop FSO is another mitigation technique proposed in literature to increase the reliability of FSO links under turbulence-induced fading channels. Here the link length between the transmitter and receiver is scaled down through Multihop routing [34]. This technique is quite common strategy in RF communication where relayed transmission provides broader and more efficient coverage. RF Multihop systems employing relayed transmission has been extensively researched in terms of the outage probability [35] - [37]. Multihop systems employ Amplify-and-Forward (AF) or Decode-and-Forward (DF) relays. AF relay systems only amplify the incoming signal and forward the signal without carrying out any form of decoding. DF relays on the other hand, decode the incoming signal and then transmit the detected version to the destination nodes.

The outage probability of a Multihop FSO link with AF or DF relays over strong turbulence fading channels is investigated in [38]. In the case of FSO systems employing AF, relays with knowledge of the CSI in the preceding hop is assumed. The authors derive a closed-form expression for the moment generating function (MGF) of the inverse end-to-end SNR. Based on this expression, the outage probability for gamma-gamma distributed channels is calculated through Laplace transform. For DF relays, the outage probability is shown to be a product of the cumulative distributed functions (CDFs) of the various point-to-point links.

The average BER is also investigated for a dual-hop FSO system employing DF relays. Simulation results show degradation in the outage probability performance with increase in the hop counts. Single hop FSO links outperform dual-hop FSO links in terms of the average BER.

ShabnamKazemlou in his work [39] introduced optical amplify-and-forward (OAF) and optical regenerate-and-forward (ORF) techniques in Multihop FSO systems to mitigate turbulence-induced fading. OAF performance is considered for two data rates (i.e. 1.25Gbps and 10Gbps) under no turbulence and weak turbulence conditions. It is shown numerically by increasing the number of OAF relays distance dependent turbulence-induced fading is mitigated. This leads to an increase in the communication distance (1.1km increment) and BER performance improvement for the same given average transmitted power but increase in background noise slows down the achievable distance improvement. ORF is further introduced to eliminate background noise and steadily increases the communication distance (1.66km better than OAF) for any relay increase. However this imposes higher complexity and increases the cost of implementation. Again the system performance is evaluated only under weak turbulence.

Multihop FSO systems improve performance in terms of coverage and transmission distance efficiency. However AF based systems suffer from increased background noise as the collected background light is accumulated at each relay during propagation whilst DF based systems suffer from increased delays [40] and system complexity.

2.4.5 Modal Compensation

Adaptive compensation of wavefront distortions has been actively under research for several years to improve the performance of optical wireless systems. In particular modal compensation involves corrections of several modes of an expansion of the total phase distortions in a set of basis functions [41].

Belmonte et al [41] studies the performance of coherent receivers employing modal compensation considering the effects of wavefront distortions and amplitude fluctuations.

Amplitude fluctuation is characterized by lognormal distribution and phase fluctuation is characterized by Gaussian distribution. The exact symbol error probability is derived for coherent detection of M-ary Phase Shift keying (M-PSK) with additive white noise. For phase fluctuations, active modal compensation technique is utilized. Two different turbulent regimes depending on the receiver aperture diameter normalized to the coherence diameter of the wavefront phase are identified. When the normalized aperture is larger, amplitude distortions becomenegligible and phase distortions become dominant. In such circumstances, higher order modes are needed to improve performance. However, when the normalized aperture diameter is relatively small, amplitude distortion becomes dominant and phase distortions have little impact on system performance. System performance becomes virtually independent of the number of modes compensated. Coherent receivers utilize both the amplitude and phase for demodulation therefore the proposed technique is insufficient to achieve substantial performance improvement.

In [42], A. Belmonte and J.M. Kahn utilize coherent fiber array consisting of densely packed multiple sub-apertures (in a hexagonalarrangement) to mitigate turbulence-induced fading. Each sub-aperture is interfaced to a single-mode fiber optic cable. Amplitude fluctuations and phase fluctuations are characterized by lognormal and Gaussian distributions respectively. The authors have identified different regimes of turbulence depending on the receiver aperture diameter normalized to the coherence diameterofthewavefront phase. When the normalized aperture is large, amplitude fluctuations become negligible and phase fluctuations become dominant. It is shown numerically that such acoherent system using field conjugation adaptive arrays with multiple sub-apertures outperforms other coherent receivers employing single monolithic-aperture receivers. The drawback of this method is that the phase fluctuations become dominant when the normalized aperture increases. Modal

compensation techniques offer some improvement but amplitudedistortions still prove problematic. Coherent systems employ both amplitude and phase for information decoding. These techniques must therefore be actively researched to address amplitude distortions for coherent systems.

2.4.6 Hybrid FSO/RF Communication

Studies have shown that both RF and FSO are not affected in the same way by atmospheric conditions. FSO links suffer significantly from atmospheric turbulence and foggy conditions [43, 44] but heavy rainfall and oxygen absorption have no significant effects. On the contrary, RF signals are susceptible to heavy rains and oxygen absorption but fog and atmospheric turbulence have no significant effects [43, 44]. Based on the complementary characteristics of FSO and RF links, researchers have proposed hybrid FSO/RF to mitigate turbulence effects.

Letzepis*et al*[45] studies hybrid FSO/RF whereby information is transmitted on both RF and FSO channels simultaneously. The paper analyzes the outage probability in high SNR regimes for cases where the receiver and/or transmitter have perfect knowledge of CSI. An optimal power allocation algorithm that minimizes the outage probability subject to peak and average power constraints is derived. Such optimal algorithm is computationally intensive. The authors address this issue by deriving a suboptimal algorithm that achieves the same power savings (tens of decibels) and minimizes the outage probability. The proposed system shows significant power savings and reduced outage probability. However the system is analyzed only under high SNR regimes and requires perfect knowledge of the instantaneous CSI at the receiver and/or transmittermaking it sophisticated to implement. Again the simultaneous transmission on both RF and FSO channels may compromise the security benefits of FSO transmissions.

To address the issue of perfect knowledge of the CSI, application of Raptor rateless codes for parallel hybrid FSO/RF transmission systems has been designed and implemented in [46]. The theoretic pertinent modulation-constrained capacity limits for FSO/RF channel is derived. Moderate-length Raptor code is shown to closely approach the limits under a variety of channel conditions. Based on the capacity expression, it is shown that the adjustment of rate *prior* to transmission will lead to rate loss and therefore rateless coding offers performance advantage over fixed-rate coding. The adopted rateless code falls into the class of hybrid automatic repeat-request (HARQ) with incremental redundancy coding; the need for sending feedback to the transmitter still remains.

N.D. Chatzidiamantis in [47] eliminates the need for feedback and implements a hybrid FSO/RF under the assumption that both MMW RF (60GHz) and FSO can support the same data rates. The proposed system transmits information over both RF and FSO channels employing PSK modulation scheme. Signals received from both links are combined in the electrical domain on a symbol-by-symbol basis using Selection Combining (SC) and Maximal Ratio Combining reception methods. Analytical approximations for BER are derived. Numerical results show hybrid FSO/RF offers significant improvement of BER over individual RF and FSO links for any given propagation distance. The drawback of this method is the parallel transmission on both channels as this may compromise the security benefits of FSO communication.

Hybrid FSO/RF links promises performance improvement of FSO links in terms of system availability and reduced BER but may compromise the security benefits associated with optical links.

2.4.7 Spatial Diversity Technique

Another promising fading mitigation technique is spatial diversity [48], a popular technique in RF communication. Spatial diversity involves the deployment of multiple receive and/or transmit apertures. Figure 2.4 shows the deployment of multiple transmitters and multiple receivers. The inherent redundant property associated with spatial diversity makes it an attractive alternate fading-mitigation technique. Besides mitigating turbulence-induced fading, multiple transmit and/or receive aperture designs have the potential to reduce the possibility of temporal blockage by obscurations (e.g. flying birds and aircraft). Further defense for the deployment of multiple transmit/receive apertures stems from limitations imposed on the maximum transmit power density (expressed in terms of milliwatts per square centimeter). The maximum amount of power that can be transmitted as safe depends on the wavelength. Higher amount of received power allows the system to support longer distances and propagation through heavier attenuation conditions whilst delivering the same data rates. Multiple copies of the transmitted optical signal are captured by the receivers and combined using selection combining (SC) or maximal ratio combining (MRC) method. SC only processes the output of the link with the highest received SNR whilst MRC processes output of all links maximizing the overall SNR.

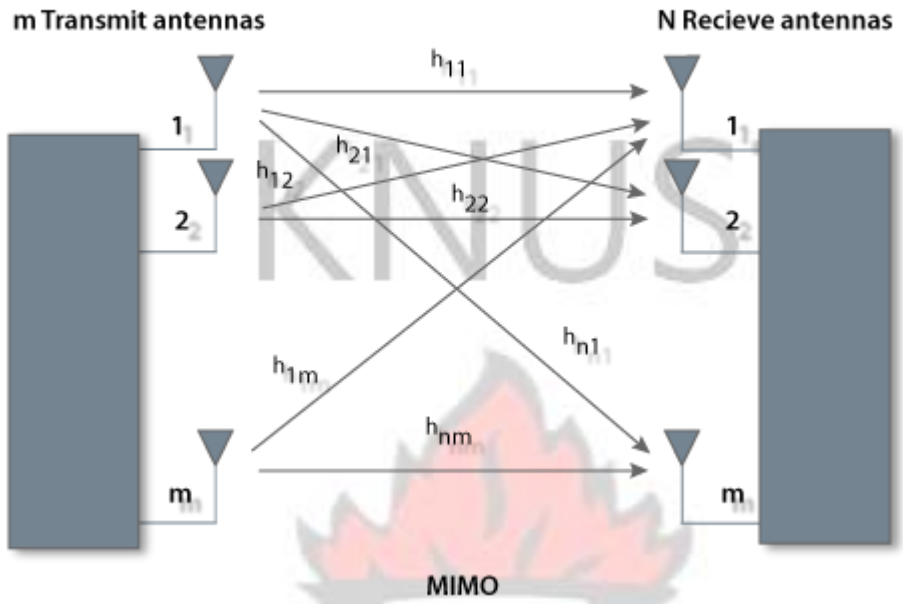

Figure 2.4 Spatial Diversity with M-transmitters and N-receivers [12]

In [49], S.M. Haas and J.H. Shapiro considered the information theoretic bounds for Multiple Input Multiple Output (MIMO). Here ergodic capacity and outage capacity are derived for FSO links employing IM/DD under lognormal turbulence-induced fading. The authors assume shot-noise-limited operation where outputs of detector are doubly Poisson stochastic processes. For high signal-to-background noise ratio, it is shown that the ergodic capacity scales as the number of transmit apertures times the number of receive apertures.

Kim et al. in [50] experimentally measures the performance of MIMO and further discusses practical design issues (such as transmitter spacing and spacing patterns) that need to be considered. They show experimentally that significant power gains can be made by employing multiple receive and/or transmit apertures.

Z. Hajjarian in [51] has also considered MIMO to mitigate turbulence-induced fading under lognormal fading channels. The authors report significant improvement in the BER when MIMO

is employed over Single Input Single Output (SISO) in the low turbulence regime. Aperture averaging for SISO and MIMO systems is also considered; it is shown to further improve the performance of MIMO than SISO systems.

Spatial diversity seems to be the most practical technique to combat turbulence-induced fading. However extensive evaluation of the performance of spatial diversity as a fadingmitigation technique has not been done. To bridge this research gap, this thesis seeks to properly evaluate the performance of spatial diversity in turbulent channels considering all regimes of atmospheric turbulence (i.e. weak, moderate and strong turbulent regimes).

2.5 Summary

Free Space Optical communication promises high data rates, license-free operation, highly secured transmission and high immunity to EMIs. Due to its high data rates, FSO can solve the last mile connectivity problem associated with microwave connectivity. However its reliability is hampered by turbulence-induced fading caused by refractive index variations of the atmosphere due to temperature and pressure inhomogeneity. As a result, powerful turbulence mitigation techniques are required to fully exploit the benefits of FSO. Error Control coding in conjunction with interleaving, Maximum Likelihood Sequence Detection (MLSD), Rate Adaptive transmission are among the proposed techniques. These techniques however have practical limitations. Spatial diversity, a popular RF technique, due to its inherent redundant property has the potential to practically combat effects of turbulence. Temporal blockage by obscurations such as flying birds can be prevented due to the inherent redundancy associated with deployments of multiple transmitters and receivers. This thesis seeks to extensively

evaluate the performance of spatial diversity in mitigating turbulenceinduced fading in terms of BER and outage probability performance metrics.

Chapter Three

Methodology

3.1 Introduction

This chapter presents the various models employed in this study. The system model for spatial diversity based FSO link is presented. Due to the randomness of atmospheric turbulence, statistical description of turbulence-induced FSO channel is presented in section 3.3. Expressions to measure the strength of atmospheric turbulence along the propagation path are derived. In section 3.4, closed-form expressions are derived to estimate the average Bit-Error-Rate (BER) for Single Input Single Output (SISO) FSO links operating over turbulent channels. Further, closed-form expressions for the average BER are derived for FSO links employing spatial diversity over atmospheric turbulent channels.

3.2 System Model

FSO system in which the message signal is sent through C transmit apertures and received by D receive apertures is considered. A discrete time ergodic channel with additive white Gaussian noise (AWGN) is assumed. Intensity Modulation/Direct Detection with On-Off Keying (OOK) and binary input and continuous output are further assumed. The optical signal received by the *dth*receiver is expressed as:

$$r_d = x \sum_{c=1}^{C} I_{cd} + w_d \qquad , d = 1,....,D \qquad \textbf{(5)}$$

Where x :the message bits with $x \in \{0,1\}$,

η :the optical-to-electrical conversion coefficient,

I_{cd} :the optical intensity from the *cth* transmit aperture to the *dth* receive aperture,

w_d : the AWGN which has zero mean and variance of $\sigma_w^2 = \frac{N_o}{2}$

N_o: Noise level

Again, it is assumed that background solar radiation noise can be neglected although it is a significantcause of interference especially in daytime. This assumption can be justified by employing photodiodes with infrared filters in practical system implementation. Furthermore, we assume that the individual FSO channels are statistically independent; this assumption can be realized by separating the individual apertures by a few centimeters because light signals have coherence length centimeters order.

3.3 Atmospheric Turbulence Channel Statistics

The optical field is defined by the modified Rytov theory proposed by Andrews *et al.* The optical field is defined as [52]-[54]:

$$U(r,L) = U_o(r,L)\exp\left[\chi_x(r,L) + \chi_y(r,L)\right] \quad \textbf{(6)}$$

Where r is the observation point in the transverse plane,

L is the length of transmission,

$U_o(r,L)$is the optical field undisturbed by atmospheric turbulence,

$\chi_x(r,L)$,$\chi_y(r,L)$are statistically independent complex disturbances resulting from large-scale and small-scale eddies respectively.

Equation (2) suggests that the optical intensity can be described by the multiplication of two independent random variables given as:

$$I = I_x I_y \qquad \textbf{(7)}$$

Where I_x and I_y are intensities resulting from large-scale and small-scale turbulent eddies respectively. Both the small-scale and large-scale intensity fluctuations are modeled using the gamma statistical model leading to the gamma-gamma statistical model [54]. The probability density function (PDF) of the turbulent-induced intensity is given by:

$$f_{I_{cd}}(I_{cd}) = \frac{2(\alpha\beta)^{(\alpha+\beta)/2}}{\Gamma(\alpha)\Gamma(\beta)} I_{cd}^{(\alpha+\beta)/2-1} K_{\alpha-\beta}\left(2\sqrt{\alpha\beta I_{cd}}\right), \; I_{cd} \geq 0 \qquad \textbf{(8)}$$

Where α, β are the parameters describing the effective number of eddies in the scattering atmosphere condition.

$\Gamma(\cdot)$ is the well-known gamma function [55],

$K_q(\cdot)$ is the modified Bessel functionof the second kind of order q [55]

The α, and β gamma-gamma parameters are related directly to atmospheric turbulence using the relationships [54]:

$$\alpha = \frac{0.49\sigma_{o2}^{2}}{\left[\exp\left(0.18 d_o^2 + 0.56\,\sigma_{12}^{7/5}\right) + 0.1\right]^{1/6}} \qquad \textbf{(9)}$$

$$\beta = \sigma_{o5}^{2}$$

□□□□exp□□(1□0.9*d* □0.051.62□*do*2/□ 5□□□□1□□□ **(10)**

□ 2 2 12

□ □ *o* *o* *o* 5) 6 □ □

Where □*o*2 □0.5*Cn*2 *k* 6 *L* 7/6 11/ **(11)**

□*kDo*2 □□2 ,

do □□□ ____4*L*

□□

□

k□□□___2□□□ : wave number of the light signal,

□ □ □

□: light wavelength, *Do* :

receive aperturediameter, *Cn*2 :

indexof refraction profile.

M : Meters.

The Hufnagel-Vally model [56] is frequently used by researchers to describe the refractive index profile. The refractive index profile, *Cn*2 ,is given by [56] as:

*C mn*2 □□ □2/3 □□□ 0.00594□□ 2721□ □□ □□ □2 10*h*5 *m*□□□exp□□□□1000_____*hm*□□□□ 2.7*10□16

exp□□□□1500_____*hm*□□□□1.7*10□14 exp□□□□100_____*hm*□□□**(12)** □

Where *h* is the height above ground. The refractive index profile is highly dependent on the height above ground. Generally, C_n^2changes from $10^{-13}m^{-2/3}$ for strong atmospheric turbulent

conditions to$10^{-17}m^{-2/3}$ for weak atmospheric turbulent conditions with $10^{-15}m^{-2/3}$ often quoted as an average value [57].

The scintillation index is used to analytically measure the atmospheric turbulence strength of the transmission channel. An expression for the scintillation index from which the strength of the atmospheric turbulence can be estimatedwill be derived. The *nth* moment of the gammagamma PDF is given in closed form by [58] as:

$$E\left[I_{cdn}\right]=\frac{\Gamma(\alpha+n)\Gamma(\beta+n)}{\Gamma(\alpha)\Gamma(\beta)} \quad \textbf{(13)}$$

The scintillation is defined as below.

$$SI=\frac{E\left[I_{cd}E_2\right]^2-E\left[I_{cd}\right]^2}{E\left[I_{cd}\right]^2} \quad \textbf{(14)}$$

$$E\left[I_{cd2}\right]=\frac{\Gamma(\alpha_2+\alpha_2+2)\Gamma(\beta_2+\beta_2+2)}{\Gamma(\alpha_2+\alpha_2)\Gamma(\beta_2+\beta_2)\Gamma(\alpha_1+\beta_1)} \quad \textbf{(15)}$$

$$E_2\left[I_{cd}\right]=\frac{\Gamma(\alpha_2+\alpha_1)\Gamma(\beta_2+\beta_1)}{\Gamma(\alpha_2)\Gamma(\beta_2)\Gamma(\alpha_1)\Gamma(\beta_1)} \quad \textbf{(16)}$$

The scintillation index is therefore derived as:

$$SI = \frac{\alpha\beta(\alpha+\beta+1)}{\alpha\beta} + 1 \qquad \textbf{(17)}$$

The scintillation index, *SI* (see equation 17) is shown to be dependent on the atmospheric parameters, αand β. These parameters represent the effective number of small-scale and large-scale scattering eddies respectively of the scattering environment. The *SI*expression derived suggests clearly that, for lower values of α and β, the atmospheric turbulence is stronger (higher SI values) and becomes weaker with increasing values of α and β.

3.3.1 Electrical Signal-to-Noise Ratio (SNR) Statistics

The instantaneous electrical SNR at the d^{th}receive aperture can be expressed as:

$$\gamma_{cd} = \frac{\eta^2 I_{cd}^2}{N_o} \qquad \textbf{(18)}$$

Further, the average electrical SNR at the d^{th}receive aperture as [5] can be defined:

$$\bar{\gamma}_{cd} = \frac{\eta^2 E^2[I_{cd}]}{N_o} \qquad \textbf{(19)}$$

The PDF of the electrical SNR, γ_{cd}, is obtained by power transformation of the random variable, I_{cd} . From equation (14), we can express I_{cd} as:

$$I_{cd} = \sqrt{\frac{\gamma_{cd} N_o}{2}}$$ And from equation (19), $\sigma^2 = \gamma_{cd} N_o$

Observe that the $E[I_{cd}] = 1$ since the I_{cd} is normalized. Again, note that μ is different from $\bar{\gamma} = E[\gamma]$ because the latter is defined as: $\bar{\gamma} = \frac{\sigma^2 E[I^2]}{\quad}$. The PDF of the electrical SNR, γ_{cd}, N_o can be obtained after the power transformation and the PDF in (8) becomes: (γ

$$f_{\gamma_{cd}}(\gamma_{cd}) = \frac{2\sqrt{\gamma_{cd}}}{2(\sigma\sigma\sqrt{\bar{\gamma}_{cd}})^{\alpha/2}\,\Gamma(\alpha)\,\Gamma(\beta)} K_{\alpha-\beta}\left(\frac{\alpha\beta\sqrt{\gamma_{cd}}}{\sigma\sqrt{\bar{\gamma}_{cd}}}\right), \quad \gamma_{cd} \geq 0 \qquad \textbf{(20)}$$

3.4 Bit-Error-Rate (BER) Analysis of Spatial Diversity Based FSO

In digital transmission, the number of bit errors is the number of received bits of a data stream over a communication channel that has been altered due to noise, interference, distortion, or bit synchronization errors. The BER is the number of bits in error divided by the total number of transferred bits during a studied time interval. Most FSO manufacturers adopt the BER as the standard performance metric. The typical BER target for most practical applications is set at 10^{-9} [59]. As a result, Monte-Carlo simulation experiments to determine this BER target

requires a large computational time; therefore analytical tools are necessary to provide comparative studies among FSO systems setups.

As mentioned earlier, atmospheric turbulence increases the BER. As a benchmark, the average BER for a Single-Input Single-Output (SISO) FSO link is derived. Expressions will be derived by employing spatial diversity at the receiver or transmitter side.

3.4.1 SISO FSO Link

Considering AWGN channel and assuming the receiver has perfect knowledge ofthe channel state information (CSI), the Bit-Error-Rate of IM/DD with On- Off-Keying is expressed as:

$$P_{BER}(e) = P(1)P(e|1) + P(0)P(e|0) \quad \textbf{(21)}$$

Where *P(1)*is the probability of transmitting a *'ON'*bitand *P(0)*is the probability of transmitting a *'OFF'*bit, *P(e|1)*is the conditional bit-error when transmitting a *'OFF'* bitand *P(e|0)* are conditional bit-error probabilities when the transmitted bit is *'ON'*bit. It is considered that there is equal probability of transmitting a '1' and a '0' (i.e. *P(0) = P(1)* (0.5). The conditional probabilities,*P(e|1)*and*P(e|0)* are equal. In the SISO link case, the indices c and d for brevity can be omitted [60]. $P_{BER}(e|I)$is given by:

$$P_{BER}(e|I) = P(e|1, I) = P(e|0, I) = Q\left(\sqrt{2NI_o}\right) \quad \textbf{(22)}$$

Where Q(.) denotes the Gaussian Q-function given by:

$$Q(x) = \frac{1}{\sqrt{2\pi}} \int_x^{\infty} e^{-t^2/2} dt \quad \textbf{(23)}$$

The Q-function can beexpressed in terms of the complementary error function(i.e. erfc)by:

$$erfc \square 2Q \square \sqrt{2}x \square$$

$$\frac{1}{2} \qquad \sqrt{} \qquad \textbf{(24)}$$

$$erfc \square Q \square 2x \square$$

$$\sqrt{2}x \square \frac{\square I}{\sqrt{2N_o}} \qquad \textbf{(25)}$$

$$x \square \frac{\square I}{2\sqrt{N_o}}$$

Therefore, we can express equation (22) as:

$$\square \; erfc$$

$$P_{BER}(e \mid I) \square Q \square \square \square \square \sqrt{2NI_o} \square \square \square \square 12 \square \sqrt{\square \square} 2 \square NI_o \square \square \square \square \quad \textbf{(26)}$$

The average BER of SISO FSO system over the turbulent atmospheric channel employing Intensity Modulation/ Direct Detection can be computed by:

$$P_{SISO}(e) \square \int_{0\square} f_I(I) \square \square \square 12 erfc \square \square \square \square 2 \square \sqrt{NI_o} \square \square \square \square \square \square \square \square \square dI \quad \textbf{(27)}$$

$$\square$$

Where $f_I(I)$is the gamma-gamma FSO channel. The integral in (23) can be obtained by expressing the modified Bessel function, $K_q(z)$and the complementary error function, $erfc(x)$ in terms of Meijer's G-functions. $K_q(z)$ and $erfc(z)$ are respectively given by [61]:

$$\sqrt{} \quad \frac{1}{2} \qquad {}_{q02\,20} \square \square \Big| \quad \square \square \square \qquad \square \qquad 1\, G_{2\,0} \square \Big|_{1} \square$$

$$z$$

$$K \square z \square \square G \square 4\,q, \square q \square \square \square \text{and} erfc \quad z \square \square \sqrt{} \square \square \square z_{0,-12} \square \square \square$$

□□
□ 2 2 □

Using these definitions,

1 2 0 □ □

K□□□(4□□I)□2G 0 2 □□□□□I | □□2□, □□2□□ □□□**(28)**

□

$erfc$□□□ □$4_2 I_2$□□□ □ 1 G 12 20 □□□□$4_2 NI_{o2}$ | 0 ,112 □□□□**(29)**

N_o□ □ □

Using equations (27) and (28), equation (29) can be expressed as:

□□□

1 □ 2□(□□□□□□)□□2 □ I□□2□□1 □□$1^2 G$ 2 0 □□□□□□I | □□2□, □□2□□ □□□□□□□□□□ 1□G 12 20

□□□□□$4_2 NI_{o2}$ | 0 1, 12 □□□□□□□□dI

$P_{SISO}(e)$□ 2□0 □ 0 2 □

(30)

By using definition [61] for integrating meijer's G-functions, closed-form relationship of equation (30) (i.e. average BER)is obtained as:

2□□□□1 2 4 □ 4□2 1□□, 2□□, 1□□, 2□□, 1□

$P_{SISO}(e)$□______4□3/ 2 □□□□□□□ G 5 2 □□□______2□2 N_0 | 2 2 2 2 0 , 1 2

□□ **(31)**

Alternatively, the average BER can be obtained by expressing equation (22) in terms of SNR,

ϒ, i.e. Q□□ □I□ □□Q□ □□ □□ 1 $erfc$□ □□□ and integrating over the SNR PDF shown in

$\sqrt{2N_o}$ □□ □□ 2 □□ 2 □□ 4 □□

□ equation (20). Thus the average Bit-Error-Rate is computed by:

$$P_{SISO}(e) = \frac{2\,\square\square\square\square_1 \quad {}_2 \quad {}_4\square\ 4\square\ {}_{1\square\square,\,2\square\square,\,1\square\square,\,2\square\square,\,1\square}}{4\square_{3/2}\,\square\square\ (\square)G\ {}_{5\,2}\,\square\square\square\ {}_2 - \square_2 \left| {}_2 \quad {}_1 \quad {}_2 \quad {}_2 \quad {}_{0,} \quad {}_2 \right.} \qquad \textbf{(32)}$$

□□

3.4.2 FSO Links employing Spatial Diversity

SISO FSO links perform poorly even in high SNR conditions. In this section, our focus will be on FSO links employing spatial diversity. Spatial diversity can be employed at either the transmit side (i.e. Multiple-Input Single-Output) or at the receiver end (i.e. Single-Input Multiple-Output) or at both ends of the channel in MIMO configuration. [60, eq. 20] gives the optimum decision metric for OOK as:

$$P(r \mid 1, I_{cd}) \underset{OFF}{\overset{ON}{\square}} P(r \mid 0, I_{cd}) \qquad \textbf{(33)}$$

Where **r**= {r_1, r_2,…,r_d} denotes the received signal vector. Studies presented by [60] can be employed for the conditional probabilities of the received vector being a ‘1’ or ‘0’. For a MIMO FSO configuration, the average BER is computed using the multidimensional integral:

$$\square\square\ \square\ {}_D\ \square\ {}_C \qquad \square_2\ \square\square$$

$$P_{MIMO}(e) = \int_{I} f_I(I) \, Q\left(\frac{C\sqrt{D}}{2N_o}\sqrt{\sum_{d=1}^{D}\sum_{c=1}^{C} I_{cd}}\right) dI \quad \textbf{(34)}$$

Where $f_I(\boldsymbol{I})$ is the joint PDF of the Gaussian vector $I_{cd} = \{I_{11}, I_{12}, \ldots, I_{CD}\}$ with size CD. Equation (34) includes the scaling factor CD to ensure fair comparison of MIMO configuration with SISO configuration. The C factor is included so that the total power of MISO transmitters is equal to the power of SISO transmitter. The factor, D is to ensure that the total receive aperture area of SIMO is equal to the area of the SISO receiver aperture. The average BER of MIMO setup in equation (34) can be obtained through numerical multidimensional integration with the help of mathematical software. However a closed-form solution is very difficult if not impossible to be obtained. To further understand the performance of FSO communication with spatial diversity, receive diversity (i.e. SIMO) and the transmit diversity (i.e. MISO) cases will be treated as special cases.

3.4.3 FSO Links employing Transmit Diversity (MISO)

Figure 3.1 shows the MISO setup. It involves C transmitters and one receiver. The total power received is summed up at the receiver end. The transmission channels for the MISO FSO link can be independent and identically distributed (i.i.d.) gamma-gamma distribution or independent and not necessarily identically distributed (i.n.i.d.) gamma-gamma distribution.

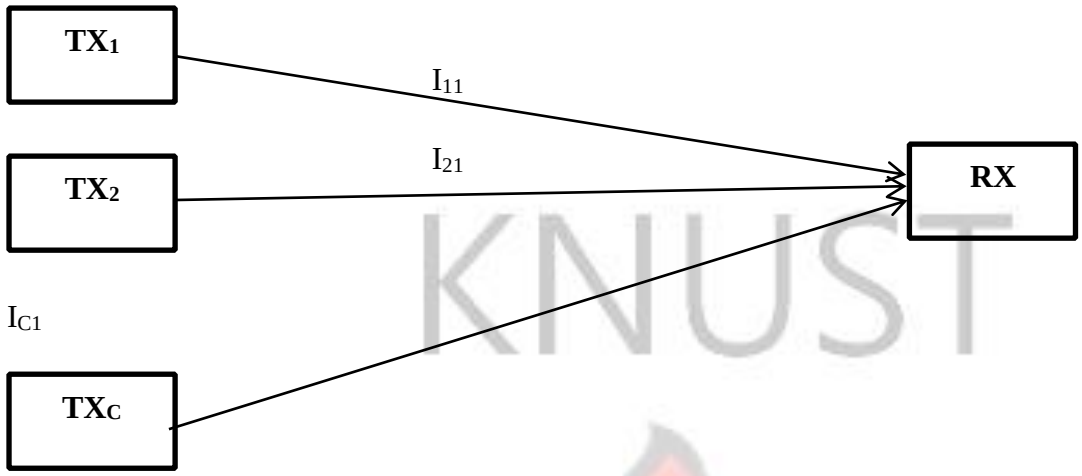

Figure 3.1 MISO configuration

For channel which is gamma-gamma i.i.d. and by implementing only transmit diversity (i.e. D=1), equation (34) can be expressed as:

$$P_{MISO}(e) = \int_{I} f_I(I)\, Q\left(\sqrt{\frac{\sum_{c=1}^{C} I_c}{2N_{o\,c}}}\right) dI \quad \textbf{(35)}$$

For i.i.d. channel, the summation, $\sum_{c=1}^{C} I_c = CI$. Equation (35) is given by:

$$P_{MISO}(e) = \int_{I} f_I(I)\, Q\left(\sqrt{\frac{CI}{2N_o}}\right) dI \quad \textbf{(36)}$$

A closed-form expression of (36) is very difficult to obtain. Therefore approximation of the Q-function presented in [60] can be employed. The Q-function approximation is given as:

$$Q(x) \approx \frac{1}{2}\left(1 - \sqrt{1 - e^{-\frac{2}{\pi}x^2}}\right) \quad \textbf{(37)}$$

$$Q(x) = \frac{e}{4} \quad 12$$

Thusthe average BER can be computed for MISO FSO systems operating over i.i.d. channel by:

$$P_{MISO}(e) = \frac{1}{12} \int_0^{\infty} f_I(I) e^{-\frac{4CN_o^2}{I^2}} dI + \frac{1}{14} \int_0^{\infty} f_I(I) e^{-\frac{3CN_o^2}{I^2}} dI \quad \textbf{(38)}$$

If the exponential function is expressed using Meijer's G-functions, the above integration is evaluated by employing Meijer's G-function integrals. The exponential function is expressed as [61]:

$$e^{-\sqrt{z}} = \frac{1}{\sqrt{\pi}} G_{00\,22}\left(4z \,\middle|\, \begin{matrix} \\ 0, \frac{1}{2} \end{matrix}\right) \quad \textbf{(39)}$$

Therefore:

$$\frac{1}{\sqrt{\pi}} \int_0^{\infty} f_I(I) e^{-\sqrt{\frac{\pi^4 I^4}{16C^2 N_o^2}}} G_{02}\left(\frac{\pi^4 I^4}{64C^2 N_o^2} \,\middle|\, \begin{matrix} 0 \\ 0, \frac{1}{2} \end{matrix}\right)$$

$$\textbf{(40)}$$

$$\frac{1}{\sqrt{\pi}} \int_0^{\infty} f_I(I) e^{-\sqrt{\frac{\pi^4 I^4}{9C^2 N_o^2}}} G_{02}\left(\frac{\pi^4 I^4}{36C^2 N_o^2} \,\middle|\, \begin{matrix} 0 \\ 0, \frac{1}{2} \end{matrix}\right)$$

The integral of equation (38) can be expressed as:

[illegible]

[illegible]

$P_{MISO}(e)$ [illegible] 2 [illegible] $((\square\square \square))$ [illegible] $\square^2$ [illegible] 121 [illegible] 12 [illegible] 1 [illegible] $\square_0 I$ [illegible] $_{02\ 02}$

[illegible] $I_{\square\square 2\square, \square\square 2\square\square}$ [illegible]

[illegible]

[illegible]

[illegible]

[illegible] 2 [illegible] $((\square\square\square))$ [illegible] $\square^2$ [illegible] 14 [illegible] 12 [illegible] 1 [illegible] $\square_0 I_{\square\square 2\square}$ [illegible] $G_{02\ 20}$

[illegible] $I|_{\square\square 2\square, \square\square 2\square\square}$ [illegible] $G_{02\ 02}$ [illegible] 36 [illegible] $C_{4\ 2} IN_{4\ o2}|_{0\ 12}$

[illegible]

[illegible]

7) **(41)**

A closed-form expression of equation (41) is obtained by employing definition [61]. The average BER is obtained by:

[illegible] 8 [illegible] $_2$ [illegible] $_o$

$P_{MISO}(e)$ [illegible] 1 [illegible] 4 [illegible] $G_{2\ 28}$ [illegible] $\overline{C^2 N}$ $(\square\square)^4 \Big|_{0,\ \frac{1}{2}}$ $\frac{4}{4}\ \frac{4}{4}\ \frac{4}{4}\ \frac{4}{4}\ \frac{4}{4}\ \frac{4}{4}\ \frac{4}{4}\ \frac{4}{4}$ C 1 [illegible], 2 [illegible], 3 [illegible], 4 [illegible], 1 [illegible], 2 [illegible], 3 [illegible], 4 [illegible] [illegible]

4 [illegible] 4

[illegible]

[illegible] 12 [illegible] 8 [illegible] 72 [illegible] [illegible] 8 [illegible] [illegible]

$_{o2}$ **(42)**

[illegible] 1 [illegible] 4 [illegible] $G_{2\ 8}$ $\overline{C^2 N}$ $(\square\square)^4 \Big|_{0,\ \frac{1}{2}}$ $\frac{4}{4}\ \frac{4}{4}\ \frac{4}{4}\ \frac{4}{4}\ \frac{4}{4}\ \frac{4}{4}\ \frac{4}{4}\ \frac{4}{4}$ C 1 [illegible], 2 [illegible], 3 [illegible], 4 [illegible], 1 [illegible], 2 [illegible], 3 [illegible], 4 [illegible] [illegible]

[illegible] 4 [illegible] 7 [illegible] 4

[illegible]

[illegible] 4 [illegible] 7 [illegible] 8 2 [illegible] $_2$ [illegible]

$P_{MISO}(e)$ [illegible] ^{12} 1 [illegible] 8 [illegible] $_7{}^2$

4 [illegible] $G_{82\ 28}$

In terms of the average SNR, [illegible]

5 2 □□□□

(43)

C

□□□1□ 4□□□ $G_{2\,8}$ □□ 4 7 □ 2 1□□, 2□□, 3□□, 4□□, 1□□, 2□□, 3□□, 4□□□□

C

1□□, 2□□, 3□□, 4□□, 1□□, 2□□, 3□□, 4□□□□

□□ □ $\frac{4\,\square}{C^2(\square\square)^4}\Big|_{0,\ \frac{1}{2}}^{\frac{4}{4}\ \frac{4}{4}\ \frac{4}{4}\ \frac{4}{4}\ \frac{4}{4}\ \frac{4}{4}\ \frac{4}{4}\ \frac{4}{4}}$ □□

□□□□4□□8□7 2 □□□□□□□□ 8 2 □□9C 2 (□□)4 0, 2 □□□□

To obtain the average BER for i.n.i.d. gamma-gamma atmospheric channel, equation (35) isstated as:

$$P_{MISO}(e)\square\ \square_{C\square} f_{I_C}(I_C)\square\square\square Q\square\square\ \square\ \square_C I_C\square\square\square\square\ {}_C dI_c \quad \textbf{(44)}$$

$$_{c\square 1}\ \square_0 \qquad \square\ \square\square C\sqrt{2N_{o\,c\square 1}}\ \square\square\square\square$$

The derived expression of equation (44) cannot be evaluated directly and therefore can only be solved through multidimensional numerical integration.

3.4.4 FSO Links employing Receive Diversity (SIMO)

The SIMO setup is illustrated in figure 3.2. A single transmitter (i.e. C=1) sends optical power and its received by multiple receivers. The transmitted optical waves are captured by several receivers and combined using selective combining (SC) or maximal ratio combining (MRC) method. SC only processes the received signal with the highest SNR whilst MRC processes output of all links maximizing the overall SNR. We will derive average BER expressions for both i.i.d. and i.n.i.d gamma-gamma channels.

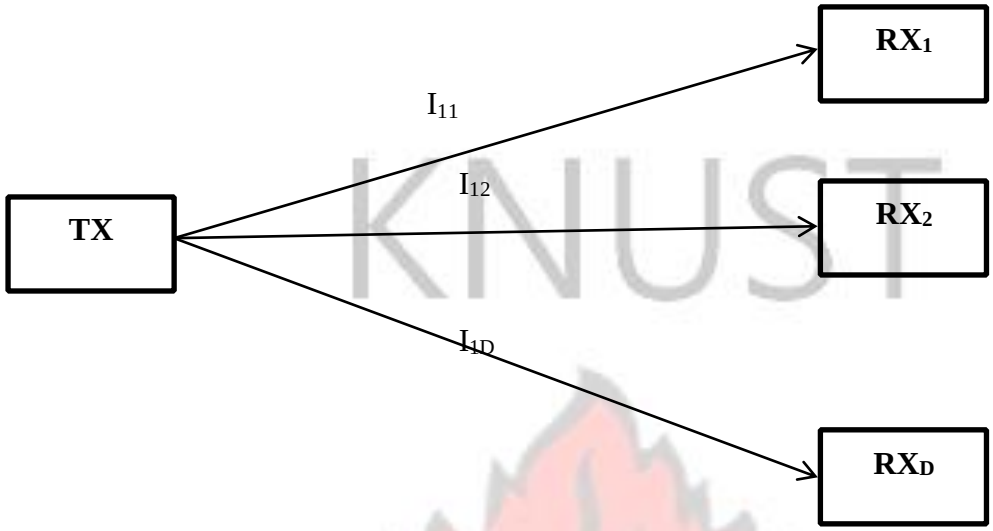

Figure 3.2 SIMO configuration

3.4.4.1 Receiver employing Selection Combining

For i.n.i.d. channel and by implementing multiple receivers, the noise variance in every N^o. For C= 1 and employing SC receiver is D times less because the noise variance is $\frac{\sigma_w}{2D}$

at the receive aperture with perfect CSI, equation (30) can be rewritten as:

$$P_{SIMO} = \int_I f_I(I)\, Q\left(\sqrt{\frac{\gamma_{d2}}{2DN_o}}\right) dI \quad \textbf{(45)}$$

Equation (41) can be further expressed for i.n.i.d. channel as:

$$P_{SIMO} = \int_{d=1}^{D} \int_{d=1}^{0} f_{Id}(I_d)\, Q\left(\sqrt{\frac{\gamma_{d2}}{2DN_o}}\right) dI_d \quad \textbf{(46)}$$

The above integral can be solved by using the Q-function approximation. Therefore,

$$P_{SIMO} \approx \frac{1}{2} \sum_{d=1}^{D} \int_0^{\infty} f_{I_d}(I_d)\, e^{-4DN_{o_d} I_d}\, dI_d \approx \frac{1}{4} \sum_{d=1}^{D} \int_0^{\infty} f_{I_d}(I_d)\, e^{-3DN_{o_d} I_d}\, dI_d \quad \textbf{(47)}$$

By writing the exponential function in terms of the Meijer's G-function and employing the relationship [61], a closed-form relation isobtained for the average BER for SC-SIMO link over i.n.i.d. as:

$$P_{SIMO}(e) \approx \frac{1}{\sqrt{\pi}} \sum_{d=1}^{D} \frac{\Gamma(4)\Gamma(4)\Gamma(4)\Gamma(4)\Gamma(4)\Gamma(4)\Gamma(4)\Gamma(4)}{\Gamma(0,\frac{1}{4})} \times G^{8,2}_{2,8}\left[\frac{\Gamma(4)\Gamma(4)\Gamma(4)\Gamma(4)\Gamma(4)\Gamma(4)\Gamma(4)\Gamma(4)}{\Gamma(0,\frac{1}{4})}\, 9D\Omega_d \,\middle|\, \begin{matrix} 1-\Omega_d, 2-\Omega_d, 3-\Omega_d, 4-\Omega_d, 1-\Omega_d, 2-\Omega_d, 3-\Omega_d, 4-\Omega_d \\ 0, \frac{1}{4} \end{matrix}\right]$$

$$\approx \frac{1}{2\sqrt{\pi}} \sum_{d=1}^{D} \frac{\Gamma(4)\Gamma(4)\Gamma(4)\Gamma(4)\Gamma(4)\Gamma(4)\Gamma(4)\Gamma(4)}{\Gamma(0,\frac{1}{4})} \times G^{8,2}_{2,8}\left[\frac{\Gamma(4)\Gamma(4)\Gamma(4)\Gamma(4)\Gamma(4)\Gamma(4)\Gamma(4)\Gamma(4)}{\Gamma(0,\frac{1}{4})}\, 9D\Omega_d \,\middle|\, \begin{matrix} 1-\Omega_d, 2-\Omega_d, 3-\Omega_d, 4-\Omega_d, 1-\Omega_d, 2-\Omega_d, 3-\Omega_d, 4-\Omega_d \\ 0, \frac{1}{4} \end{matrix}\right] \quad \textbf{(48)}$$

For i.i.d. random variable, I_d, equation (34) can be rewritten as:

$$P_{SIMO}(e) \approx \int_I f_I(I)\, Q\left(\sqrt{2N_o I}\right) dI \quad \textbf{(49)}$$

Since summation, $\sum_{d=1}^{D} I_d = I$.

$d \square 1$

The expression (49) is exactly equal to the expression (36) of the MISO case for the i.i.d. channel. Therefore the solution to expression (36) also holds for expression (49) above. Thus a closed-form relationship for the average BER for SC-SIMO over i.i.d. channel is expressed as:

$$\square\square 1 \square \quad 4\square\square \quad 28 \square \quad \frac{4 \square}{D^2 (\square\square)^4} \Big| \; 0, \frac{1}{2} \quad D \quad 5 \quad 2$$

$$P_{SIMO}(e) \square\square\square \quad \square \quad G_{82} \square\square\square\square\square\square\square \; \square$$

$$\square\square\square 12\square 8\square \; 2 \square\square\square\square\square\square\square \quad \square\square$$

$$\square\square\square\square 1\square\square \quad 4\square\square \; G_{28} \square\square \quad 4_7 \square_2 \; 4 \Big| \; 1\square\square, 2\square\square, 3\square\square, 4\square\square, 1\square\square, 2\square\square, 3\square\square, 4\square\square \square\square\square \quad D$$

$$\square\square\square^4 \square 8 \square_7^2 \square\square\square\square\square\square\square_{82} \square 9D_2 (\square\square) \quad 0, \quad 2 \qquad \square\square\square\square \quad \textbf{(50)}$$

3.4.4.2 Receiver employing Maximal Ratio Combining

When the receiver employs MRC detection, all the received intensities at the individual receivers are added. Equation (34) is rewritten as:

$$P_{SIMO}(e) \square \square_I f_I(I) \; Q \square \square\square \; D \sqrt{2 \; N_o} \square_{d^D \square 1} I_d \square\square \square \; dI \quad \textbf{(51)}$$

It is observed that the derived expression above is exactly the same as the MISO case for both i.i.d. and i.n.i.d. gamma-gamma distribution. Therefore derived expressions for the MISO

scenario also hold for the MRC-SIMO. It can be concluded that a closed-form expression for i.i.d. is:

$$D$$

$$P_{SIMO}(e)\square\square\square\square\square\square\square 12\; 1\;\square\square\square 8\square_{7}{}^{2}\; 4\square\square\square\square\square\square\square\square\square\square G_{8\,2}{}^{2\,8}\square\square\square\square$$

$$\frac{4\;\square}{D^{2}\,(\square\square)^{4}}\left|\begin{matrix}\frac{}{4} & \frac{}{4} & \frac{}{4} & \frac{}{4} & \frac{}{4} & \frac{}{4} & \frac{}{4} & \frac{}{4}\\ 0, & \frac{1}{2} & & & & & 5 & 2\end{matrix}\right. \quad 1\square,$$

$$2\square,\,3\square,\,4\square,\,1\square,\,2\square,\,3\square,\,4\square\square\square\square\square\square\square\square\;\square$$

$$D$$

$$\square\square 1\square \qquad 4\square\square\square\, G_{2\,8}\square\square \qquad 4_{7}\square_{2}\left|\begin{matrix}1\square, & 2\square\square, & 3\square\square, & 4\square\square, & 1\square\square, & 2\square\square, & 3\square\square, & 4\square\square\end{matrix}\right.\square\square\square\square \quad \frac{1}{}$$

$$\square\square\square\square\square 4\square\square 8_{72} \qquad 8\,2\,\square\square 9D_{2}\,(\square\square)_{4} \quad 0, \quad 2 \qquad \square\square\square\square \quad \textbf{(52)}$$

$$\square\;\square\square\square\square\square\square\square\square$$

Similar to the MISO FSO link over i.n.i.d. channel, the closed-form expression for MRCSIMO FSO link is impossible to be derived and therefore a multidimensional numerical integration must be utilized.

3.5 Summary

The scintillation index, SI, describes the strength of IRT along the propagation path of FSO links. In this section, we have derived mathematical expression for the SI using the PDF of gamma-gamma distribution. The scintillation index was shown to be strongly dependent on the gamma-gamma parameters, α and β. The effect of SI on the average BER of FSO links was described. Mathematical expressions were derived to estimate the average Bit-Error-Rate for SISO FSO systems as a benchmark for comparison. To have detailed knowledgeof the

performance of spatial diversity based FSO links, closed-form relationships have been derived for MISO and SIMO links in terms of the Bit-Error-Rate.

Chapter 4

Results and Discussions

4.1 Introduction

In the preceding chapter, the system model was discussed to derive mathematical relationships for the scintillation index and the average BER. This chapter presents results for the thesis. The statistical description of FSO links over turbulent channels is presented with the aim of estimating the strength of turbulence in terms of the scintillation index. The average BER of the different configurations of FSO links employing Spatial Diversity is presented.

4.2 Scintillation Index

Scintillation index describes the strength of atmospheric turbulence along the propagation path of FSO links. Due to the random nature of atmospheric parameters, we have characterized the scintillation index by employing the gamma-gamma statistical model. The parameters of the gamma-gamma model, α and β are related to atmospheric parameter, β_o. α and β are the gamma-gamma parameters that characterize large and small-scale eddies respectively.

Figure 4.1 shows the relationship between the atmospheric parameter, β_o and gamma-gamma parameters, α and β using equations (9) and (10). Optical wavelength of 1550nm; a propagation

length, L of 2km and the receiver diameter, D_o of 5cm were used. The parameters, α and β reduce as the turbulent atmospheric condition parameter, β_o increases. Increase in the β_o-parameter means increment in the IRT strength along the transmission path.

Therefore higher values of the gamma-gamma parameters, α and β means the atmospheric turbulence is low and vice-versa.

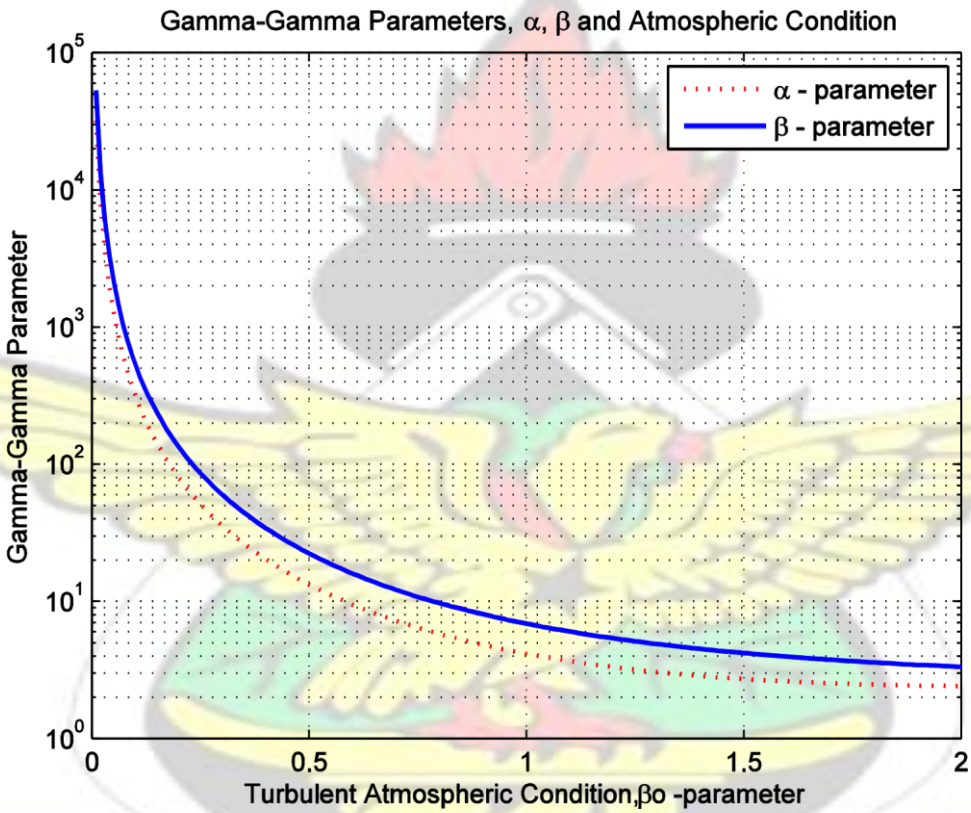

Figure 4.1 Relationship between Atmospheric parameter,β_o and GG parameters α and β

Based on the gamma-gamma parameters,α and β, we derived an expression for the SI that measures the strength of atmospheric turbulence along the propagation path. Figure 4.2 shows the relationship between the SI and the gamma-gamma parameters,α and β. The βparameter is fixed at β = 1 whilst theα-parameter is varied. The SI reduces as α-parameter increases. The β-

parameter is then fixed at β = {5, 10, 20} whilst the α-parameter is varied. In all scenarios, the SI reduces with increase in α-parameter. For example, when α = 1 and β = 1, SI of 3 is obtained. When α = 1 and β = 5, SI of 1.4is obtained. Thusasα and β parameters increase, the SI reduces and vice-versa. This is consistent with the relationship between the β_o-parameter and the gamma-gamma parameters, α and β. As the atmospheric condition parameter, β_o-parameter increases, α and β parameters reduceand the SI increases. Higher values of SI mean higher atmospheric turbulence along the propagation path.

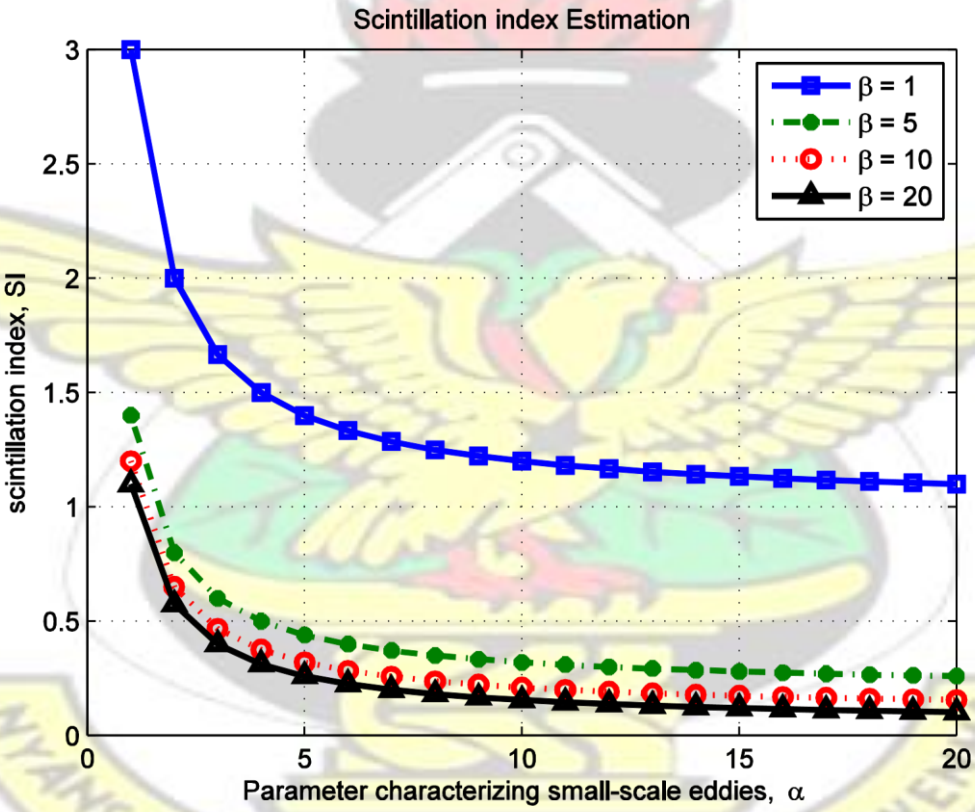

Figure 4.2 Scintillation Index, SI as a function of gamma-gamma parameters, α and β

4.3 Average BER for SISO FSO Link

For the purpose of comparison, a closed-form relationship estimating the average BER of a

SISO FSO link over a turbulent gamma-gamma channel was derived. The average BER of SISO FSO link in terms of the SI using equation (32) is shown in figure 4.3.

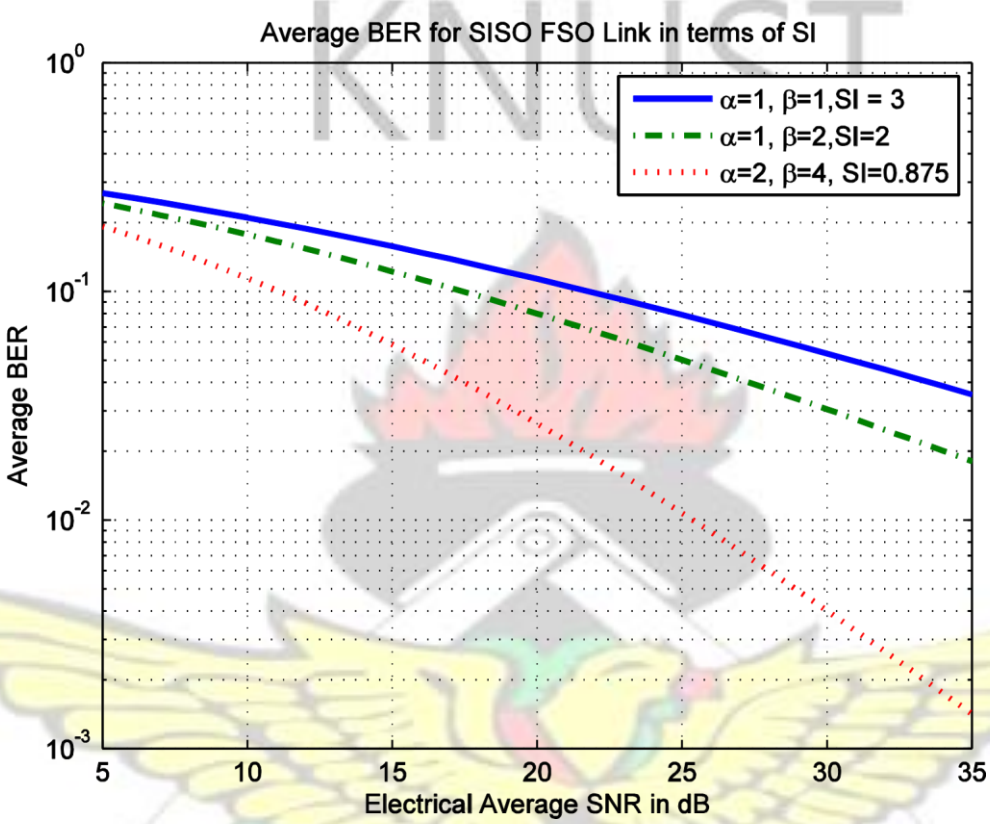

Figure 4.3 Average BER of SISO FSO link in terms of SI

When $\alpha = 1$ and $\beta = 1$, SI = 3, the average BER obtained for an electrical average SNR of 5dB was higher than 0.1. The average BER reduces as the electrical average SNR increases as expected. At high electrical average SNR of 35dB, the average BER reduces below 0.1.

When the SI reduces to 2, the average BER obtained for an electrical average SNR of 5dB was still higher than 0.1 but the average BER was lower than when SI = 3. Again as the electrical average SNR increases, the average BER reduces significantly. Increasing values of SI means

stronger atmospheric turbulence along the propagation path. As expected, as the SI increases, the average BER increases thus reducing the system performance of the FSO link.

Even at very high electrical average SNR, the system fails to achieve the desired average BER (i.e. 10^{-9}) of wireless networks.Generally, the average BER reduces as the average SNR increases and the average BER increases as the SI increases.

As observedin figure 4.3, the average BER of SISO FSO links is very high even at high SNR conditions. This is undesirable in wireless communication systems. Therefore effective techniques are required to reduce the effect of atmospheric turbulence on the FSO link.

Spatial diversity is therefore employed to combat the effect of atmospheric turbulence.

4.4 Average BER for FSO Links employing Transmit Diversity

As seen in the previous section, the average BER for SISO FSO links is very high. This is undesirable. Transmit diversity is employed and closed-form relationships estimating the average BER for optical links with transmit diversityare derived.

Figure 4.4 shows the average BER for MISO links over i.i.d. gamma-gamma channel using equation (43). The gamma-gamma parameters of $\alpha = 2$ and $\beta = 4$are used. Graphs for transmit apertures of C = {2, 3, 4, 5, 6} are plotted. For the purpose of comparison between SISO FSO links and MISO FSO links, a graph for SISO FSO links has been included in the plot. As shown in the graph, the SISO fails to achieve the target BER (i.e. 10^{-9}) of wireless communication systems even at high SNR conditions. The BER performance is

substantiallyenhanced when the quantity of transmitters are increased. With a target BER of 10^{-5}, the SISO FSO link requires SNR of 65dB. The same average BER target can be achieved

at an average SNR of 40dB with only two transmit apertures. Increasing transmitter quantity results in substantial reduction in the average BER and the average SNR gain increases significantly. With six transmit apertures, a target average BER of 10^{-5} can be achieved at average SNR of 24dB. This is significant improvement over the SISO case. The desired average BER of 10^{-9} can be achieved with five transmit apertures at average SNR of 34dB. MISO FSO configuration significantly improves the BER performance of optical links over turbulent channels.

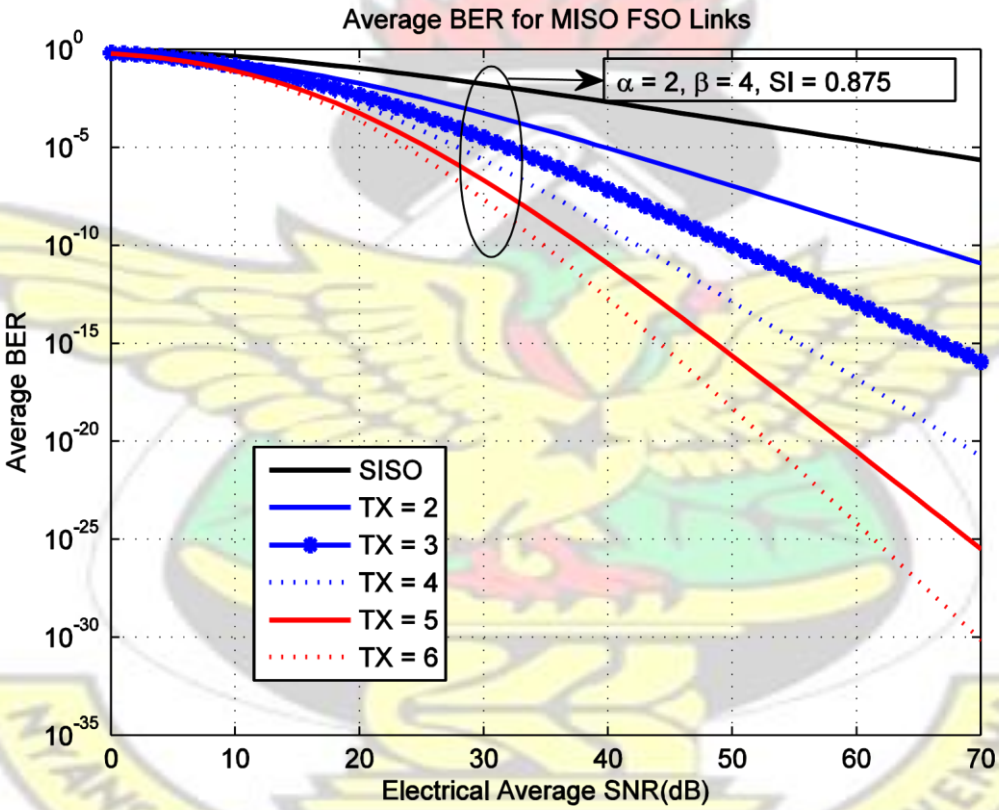

Figure 4.4 Average BER for MISO FSO Link over i.i.d. channel with α = 2 and β = 4

4.5 Average BER for FSO Links employing Receive Diversity

Furthermore, closed-form expressions have been derived for FSO links employing multiple receive apertures. When receive diversity is employed, the system can use either Maximum

Ratio Combining or Optimal Combining detection techniques. Closed-form expressions are obtained for both i.i.d. and i.n.i.d. gamma-gamma distributions when SC detection technique is used. It is observed that the solution for the MRC case was exactly the same as the MISO case for both i.i.d. and i.n.i.d. gamma-gamma distribution.

Figure 4.5 shows the average BER for OC-SIMO FSO link over i.i.d. gamma-gamma channel. The atmospheric parameters, $\alpha = 1$, $\beta = 2$are used. The Scintillation Index is 2. Similar to the MISO case, the average BER reduces with increase in the number of receive apertures. A target BER of 10^{-5} was obtained at an average SNR of 45dB with four receive apertures. The same average BER target of 10^{-5} was achieved at average SNR of 36dB showing significant gain over the four receive apertures case.

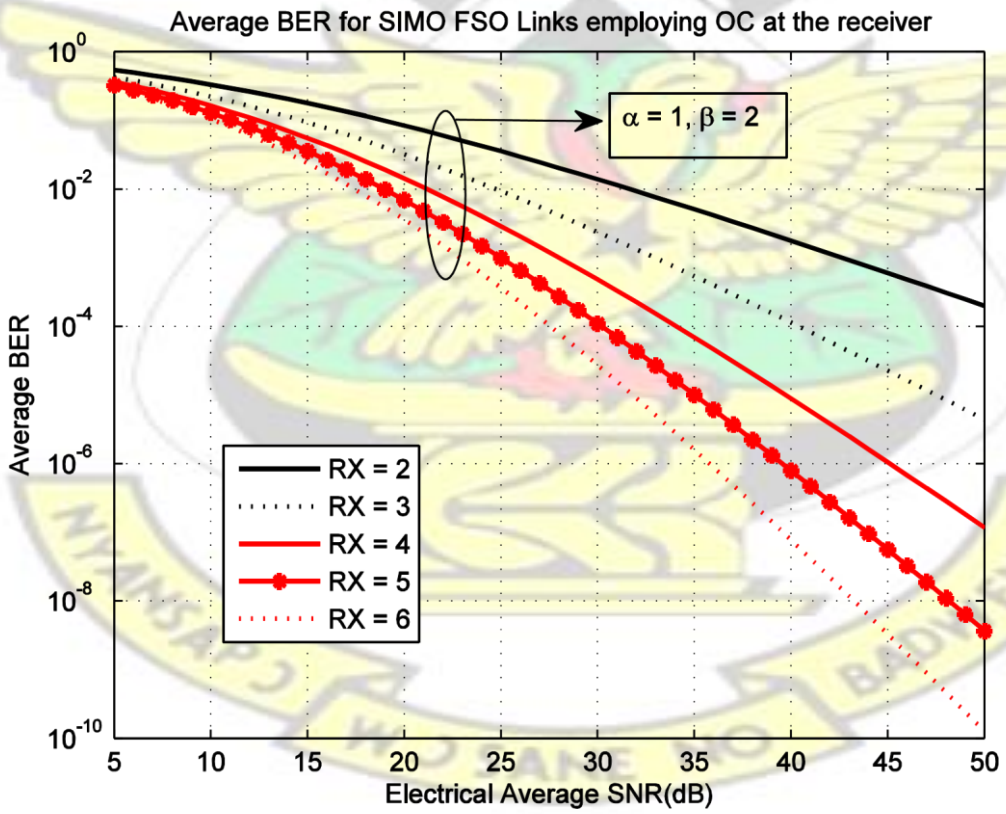

Figure 4.5 Average BER of OC-SIMO,$\alpha = 1$, $\beta = 2$.

Figure 4.6 shows the average BER for SIMO link employing OC detection technique over i.n.i.d. channel. We considered three cases with the number of receive apertures, D ranging from two to four. For the two receivers case, we used atmospheric parameters, α_1= 1 and β_1 = 1 for the first link and α_2 = 1 andβ_2 = 2 for the second link and $\mu = \{\mu_1 = \mu, \mu_2 = 2\mu\}$. Atmospheric turbulence on the first link (i.e. SI = 3) was higher than the second link (SI = 2). For an average SNR of 50dB, a BER of 10^{-4} was obtained. For the three receivers case, we used the atmospheric parameters, $\alpha = \{1, 1, 2\}$ and $\beta = \{1, 2, 4\}$ and $\mu = \{\mu_1 = \mu, \mu_2 = 2\mu, \mu_3 = 4\mu\}$. An average BER below 10^{-5} was obtained at an average electrical SNR of 50dB. Moreover, we employed four receive apertures. The following atmospheric parametersare used:

$\alpha = \{1, 1, 2, 4\}$, $\beta = \{1, 2, 4, 8\}$ and $\mu = \{\mu_1 = \mu, \mu_2 = 2\mu, \mu_3 = 4\mu, \mu_4 = 8\mu\}$. A far lower average BER of 10^{-15} was obtained at an average SNR of 50dB. The desirable BER of $10^{9}$was obtained at an average SNR of 34dB.This is because the resultant effect of scintillation on the links reduces due to the SI of the fourth link being significantly lower than the remaining links.

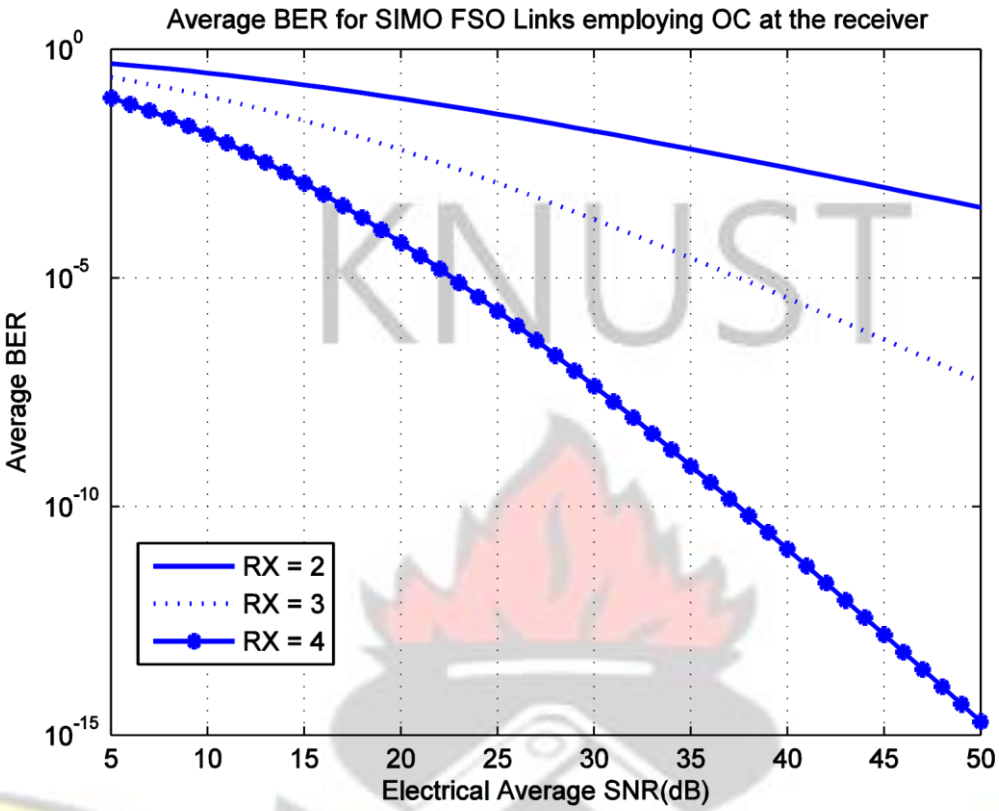

Figure 4.6 Average BER of OC-SIMO FSO Link over i.n.i.d. gamma-gamma channel. For D = 2 :(α= 1, 1; β= 1, 2; $\mu_1 = \mu$, $\mu_2 = 2(\mu)$), D = 3 :(α= 1, 1,2; β= 1, 2, 4; $\mu_1 = \mu$, $\mu_2 = 2(\mu)$,$\mu_3 = 4(\mu)$) and D = 4 :(α= 1, 1, 2, 4;β = 1, 2, 4, 8; $\mu_1 = \mu$, $\mu_2 = 2(\mu)$,$\mu_3 = 4(\mu)$,$\mu_4 = 8(\mu)$).

Closed-form expressions are derived for SIMO employing MRC detection technique. It should be emphasized here that, the derived expressions for the MRC-SIMO was exactly equal to the MISO case. It can therefore be concluded that the results and analysis for the

MISO case also holds for MRC-SIMO case.

Chapter 5

Conclusion and Recommendation

5.1 Conclusion

Free Space Optical (FSO) communication is the transmission of high rate data using optical signals through the atmosphere. Thus it is a wireless communication system. This technology has the potential to provide high speed data (i.e. gigabits data) transmission and license-free operation. Again, FSO promises highly secured transmission and high immunity to electromagnetic interference with low probability of interception and low probability of detection (LPI/LPD) properties. However FSO communication's potentials are limited by atmospheric conditions such as index-of-refraction turbulence (IRT), aerosol scattering and absorption. IRT reduces the performance of FSO communication systems by increasing the Bit-Error Rate (BER). Therefore more powerful mitigation techniques are required to reduce the impact of atmospheric turbulence on FSO links. Rate Adaptive transmission, hybrid RF/FSO, Error Control Coding with interleaving, MLSD, Modal Compensation and Spatial Diversity are among techniques suggested in literature to mitigate negative effects of IRT. Amongst all these mitigation techniques, spatial diversity appears to be the most practical technique to combat the effects of IRT.

In this thesis, the performance of spatial diversity based links has been investigated. Due to the randomness of IRT phenomenon, atmospheric turbulence ischaracterized using the PDF of the gamma-gamma statistical distribution. The gamma-gamma distribution is chosen because of its ability to model multiple scattering arising from both small-scale and largescale eddies (i.e.

both weak and strong turbulence conditions). Again, the gamma-gamma parameters can be related to atmospheric parameters with simple expressions.

Scintillation Index, a statistical measure of atmospheric turbulencehas been shown to depend strongly on the gamma-gamma parameters, α and β. These parameters are related to atmospheric turbulent conditions. From the results obtained, both α and β decrease with increase in the β_o-parameter (parameter characterizing atmospheric turbulence). It has been shown that as α and β decrease, the SI increases and thus the atmospheric turbulence increases along the transmission channel.

Moreover, we have investigated the effect of atmospheric turbulence on SISO FSO links in terms of the average BER. Highly accurate closed-form mathematical expressions for the average BER of SISO FSO links have been derived as a benchmark. Generally, the average BER reduces as the electrical average SNR increases and vice-versa. When the SI reduces, the average BER reduces. At SI of 3, an average BER less than 10^{-1} is obtained at average SNR of 35dB. As SI reduces to 0.875, the average BER reduces significantly to 10^{-3} for the same electrical average SNR (i.e. 35dB). However the system fails to achieve the desired average BER of 10^{-9} required from wireless communication systems even at very high SNR conditions. This gives credence to the necessity to employ multiple receive and/or transmit apertures.

Furthermore, we have derived highly accurate closed-form expressions for the average BER of FSO links with multiple receive and/or transmit apertures. Closed-form expressions have been derived for both independent and identically distributed (i.i.d.) and independent not necessarily identically distributed (i.n.i.d.) gamma-gamma channels. Numerical results obtained show that the average BER reduces significantly when the number of receive and/or transmit apertures are increased. Closed-form expressions for Multiple Input Single Output (MISO) FSO

linkshave been derived. The average BER reduces significantly as the number of transmit apertures increase at all SNR conditions. Further closed-form expressions have been derived by employing the Single Input Multiple Output (SIMO) configurations. Both Maximum Ratio Combining (MRC) and Selective Combining (SC) detection techniques have been considered. For SIMO configurations, the average BER reduces as the number of receive apertures increase as in the MISO case. It can be concluded here that both MISO and

SIMO yield similar average BER performance. Therefore any of the two configurations (i.e. SIMO and MISO) can be employed to mitigate turbulence-induced fading.

5.2 Recommendation

From the results obtained in this thesis, spatial diversity promises significant average BER performance for FSO links over both strong and weak turbulent channels. Practical implementation of spatial diversity based FSO links are therefore required to have further insight into the performance of spatial diversity based FSO communication systems on turbulent channels. Again, research on spatial diversity based FSO links considering the combined effects of atmospheric turbulence and atmospheric scattering needs to be conducted.

References

[1] D. Kedar and S. Arnon, "Urban Optical Wireless Communication Networks: the main challenges and possible solutions," IEEE Communications Magazine, vol. 42, no. 5, pp.S2–S7, May 2004.

[2] L.C. Andrews, R.L. Phillips, C.Y. Hopen, "Laser Beam Scintillation with Applications" SPIE Press, Washington, 2001.

[3] H. Henniger, O. Wilfert, "Introduction to Free Space Optical communications" Radioengineering, vol. 19 Jun. 2010 pp. 203.

[4] F. Liu, U. Vishkin, and S. Milner, "Bootstrapping free-space optical networks," IEEE J. Sel. Areas Communications., vol. 24, no. 12, pp. 13–22, Dec. 2006.

[5] X. Zhu, J.M. Kahn, "Free Space Optical Communication through Atmospheric Turbulence Channels", IEEE Transactions on Communication, vol. 50, No. 8, August 2002.

[6] D. Sadot, A. Melamed, and N. S. Kopeika, "Effects of aerosol forward scatter on the long- and short-exposure atmospheric coherence diameter, "Waves in Random Media, vol. 4, no. 4, pp. 487–498, Oct. 1994.

[7] S. Arnon and N. S. Kopeika, "Effect of particulates on performance of optical communication in space and an adaptive method to minimize such effects," Appl. Opt., vol. 33, no. 21, pp. 4930–4937, July 1994.

[8] J.M. Kahn, "Markov chain model in maximum-likelihood sequence detection for freespace optical communication through atmospheric turbulence channels," IEEE Trans. Commun., no. 3, 2003.

[9] M. Uysal, S. M. Navidpour, and J. T. Li, “Error rate performance of coded free-space optical links over strong turbulence channels” IEEE Commun. Lett., vol. 8, pp. 635–637, Oct. 2004.

[10] X. Zhu and J.M. Kahn, “Performance bounds for coded free-space optical communications through atmospheric turbulence channels,” IEEE Trans. Commun., vol. 51, pp. 1233–1239, Aug. 2003.

[11] D. Killinger, "Free space optics for laser communication through the air," Optics & Photonics News, vol. 13, pp. 36-42, Oct. 2002.

[12] “Free Space Optics- FSO”, http://www.surajinformatics.com/fso-free-space-optics.htm, last visited: 29/08/2014.

[13] Z. Bielecki, B. Kolosowski, J. Mikolajczyk, “Free Space Optical Data Link using quantum cascade laser”.

[14] W.O. Popoola, “Subcarrier intensity modulated Free Space Optical Communication Systems.” PhD dissertation, University of Northumbria, Newcastle, 2009.

[15] Z. Chen, S. Yu, T. Wang, G. Wu, S. Wang, W. Gu, “Channel correlation in aperture receiver diversity systems for free-space optical communication,” Journal of Optics, vol. 14, Number 12.

[16] W. K. Pratt, Laser Communication Systems, 1st ed. New York: John Wiley & Sons, Inc., 1969.

[17] G.R. Osche, Optical Detection Theory for Laser Applications. New Jersey: Wiley, 2002. [18] K. Kiasaleh, “Performance of coherent DPSK free-space optical communication

systems in K-distributed turbulence," IEEE Trans. Commun., vol. 54, no. 4, pp. 604–607, Apr. 2006.

[19] H.G. Sandalidis, T.A. Tsiftsis, G.K. Karagiannidis, M. Uysal,"BER Performance of FSO Links over Strong Atmospheric Turbulence Channels with Pointing Errors," IEEE Commun. Letters, vol. 12, No. 1, January 2008.

[20] M. Uysal and J. T. Li, "BER performance of coded free-space optical links over strong turbulence channels," in Proc. IEEE Vehicular Technological Conference (VTC spring), May 2004, pp. 168–172.

[21] A. Goldsmith and S. Chua, "Adaptive coded modulation for fading channels," Communications, IEEE Transactions on, vol. 46, no. 5, pp. 595–602, 1998.

[22] M. S. Alouini and A. J. Goldsmith, "Adaptive moulation over Nakagami fading channels," Wireless Personal Communications, vol. 13, no. 1-2, pp. 119–143, May 2000.

[23] Chatzidiamantis, N. D., Lioumpas, A. S., Karagiannidis, G. K. & Arnon S. [2011], "Adaptive subcarrier PSK intensity modulation in free space optical systems", IEEE Trans. Commun. 59 (5): 1368–1377.

[24] W.G. Cowley, K.D. Nguyen, D. Giggenbach, "Adaptive Symbol-Rate Free-SpaceOptical Communications", IEEE 2013 Australian Communications Theory Workshop (AusCTW), pp.122-127.

[25] A. Garcia-Zambrana, C. Castillo-Vazquez, and B. Castillo-Vazquez, "Rate-adaptive FSO links over atmospheric turbulence channels by jointly using repetition coding and silence periods", 22 November 2010 / Vol. 18, No. 24 / OPTICS EXPRESS 25422.

[26] A. Garcıa-Zambrana, “Error rate performance for STBC in free-space optical communications through strong atmospheric turbulence”, IEEE Commun. Lett.11 (5), 390– 392 (2007).

[27] A. Garcia-Zambrana, C. Castillo-Vazquez, B. Castillo-Vazquez, and A. HiniestaGomez, “Selection Transmit Diversity for FSO Links Over Strong Atmospheric Turbulence Channels,” IEEE Photon. Technol. Lett.21 (14), 1017–1019 (2009).

[28] A. Garcıa-Zambrana, C. Castillo-Vazquez, and B. Castillo-Vazquez, “Space-time trellis coding with transmit laser selection for FSO links over strong atmospheric turbulence channels,” Opt. Express 18(6), 5356–5366 (2010).

[29] N. D. Chatzidiamantis, A. S. Lioumpas, G. K. Karagiannidis, and S. Arnon, “Optical Wireless Communications with Adaptive Subcarrier PSK Intensity Modulation,” (2010) Accepted for publication in IEEE Global Telecommunications Conference (GLOBECOM ’10), URLhttp://users.auth.gr/nestoras.

[30] X. Zhu and J.M. Kahn, “Pilot-symbol assisted modulation for correlated turbulent freespace optical channels", in Proc. SPIE Intl. Symp. Optical Science Technol., San Diego, CA, 2001.

[31] M. L. B. Riediger, R. Schober, and L. Lampe, “Fast multiple-symbol detection for freespace optical communications," IEEE Trans. Commun.,vol. 57, no. 4, pp. 1119-1128, Apr. 2009.

[32] X. Zhu and J.M. Kahn, “Markov Chain Model in Maximum-Likelihood Sequence

Detection for Free-Space Optical Communication through Atmospheric Turbulence Channels", IEEE transactions on communications, VOL. 51, NO. 3, MARCH 2003, pp. 509 516.

[33] N.D. Chatzidiamantis, G.K. Karagiannidis, and M. Uysal, "Generalized MaximumLikelihood Sequence Detection for Photon-Counting Free Space Optical Systems", IEEE transactions on communications, vol. 58, no. 12, December 2010, pp. 3381-3385.

[34] A. S. Acampora and S. V. Krishnamurthy, "A broadband wireless access network based on mesh-connected free-space optical links," IEEE Personal Communications, vol. 6, pp. 62– 65, Oct. 1999.

[35] M. O. Hasna and M. S. Alouini, "Outage probability of multihop transmission over Nakagami fading channels," IEEE Commun. Lett.,vol. 7, pp. 216–218, May 2003.

[36] G. K. Karagiannidis, D. A. Zogas, N. C. Sagias, T. A. Tsiftsis, and P. T. Mathiopoulos, "Multihop communications with fixed-gain relays over generalized fading channels," in Proc. IEEE Global Telecommunications Conference (GLOBECOM '04), vol. 1, Dallas Texas, USA, Dec. 2004, pp. 36–40.

[37] G. K. Karagiannidis, T. A. Tsiftsis, and R. K. Mallik, "Bounds for multihop relayed communications in Nakagami-m fading," IEEE Trans. Commun., vol. 54, pp. 18–22, Jan. 2006.

[38] T.A. Tsiftsis, H.G. Sandalidis, G.K. Karagiannidis, and N.C. Sagias, "Multihop FreeSpace Optical Communications over Strong Turbulence Channels", in the IEEE ICC 2006 proceedings, pp. 2755 – 2759, 2006.

[39] S. Kazemlod, "All-Optical Multihop Free-Space Optical Communication Systems", Master of Applied Science, McMaster University, October 2010.

[40] J. Akella, M. Yuksel, S. Kalyanaraman, "Error Analysis of Multi-Hop Free-Space Optical Communication", in Proc. of IEEE International Conference on Communications 2005 (ICC'05), Seoul, Korea, May 2005.

[41] A. Belmonte, J.M. Kahn, "Performance of synchronous optical receivers using atmospheric compensation techniques", OPTICS EXPRESS 14151, Vol. 16, No. 18, 1 September 2008.

[42] A. Belmonte, J.M. Kahn, "Field Conjugation Adaptive Arrays in Free-Space Coherent Laser Communications", J. Opt. Commun. Netw./ Vol. 3, No. 11/November 2011.

[43] F. Nadeem, V. Kvicera, M. Awan, E. Leitgeb, S. Muhammad, and G. Kandus, "Weather effects on hybrid FSO/RF communication link, "IEEE J. Sel. Areas Commun., vol. 27, no. 9, pp. 1687–1697, Dec. 2009.

[44] H. Wu and M. Kavehrad, "Availability evaluation of ground-to-air hybrid FSO/RF links", Int. J. of Wir. Inf. Networks, vol. 14, no. 1, pp. 33–45, Mar. 2007.

[45] N. Letzepis, K.D. Nguyen, A.G. Fabregas, and W.G. Cowley, "Hybrid Free-Space Optical and Radio-Frequency Communications: Outage Analysis", IEEE, ISIT 2010, Austin, Texas, U.S.A., June 13 - 18, 2010, pp.2048-2052.

[46] A. AbdulHussein, A. Oka, T.T. Nguyen and L. Lampe, "Rateless Coding for Hybrid Free-Space Optical and Radio-Frequency Communication", IEEE Transactions On Wireless Communications, VOL. 9, NO. 3, March 2010, pp. 1-7.

[47] N.D. Chatzidiamantis, G.K. Karagiannidis, E.E. Kriezis and M. Matthaiou, "Diversity Combining in Hybrid RF/FSO Systems with PSK Modulation", 2011 IEEE International Conference on Communications (ICC), Kyoto, June 2011, pp. 1-6.

[48] A. Paulraj, R. Nabar, and D. Gore, Introduction to Space-Time Wireless Communications. Cambridge, UK: Cambridge University Press, 2003.

[49] S. M. Haas and J. H. Shapiro, "Capacity of wireless optical communications," IEEE J. Select. Areas Commun., vol. 21, no. 8, pp. 1346-1357, Oct. 2003.

[50] I. Kim, H. Hakakha, P. Adhikari, and E. J. Korevaar, "Scintillation reduction using multiple transmitters," in Proc. SPIE, Feb. 1997, vol. 2990.

[51] Z. Hajjarian, J. Fadlullah, M. Kavehrad, "MIMO Free Space Optical Communications in Turbid and Turbulent Atmosphere", Journal of Communications, Vol. 4, No. 8, September
2009, pp. 524-532.

[52] L. C. Andrews, R. L. Phillips, C. Y. Hopen and M. A. Al-Habash, "Theory of optical scintillation", Journal of Optical Society America A, vol. 16, no.6, p. 1417-1429, June 1999.

[53] L. C. Andrews, R. L. Phillips and C. Y. Hopen, "Aperture averaging of optical scintillations: Power fluctuations and the temporal spectrum", Waves Random Media, vol. 10, p. 53-70, 2000.

[54] M. A. Al-Habash, L. C. Andrews and R. L. Phillips, "Mathematical model for the irradiance probability density function of a laser beam propagating through turbulent media", Optical Engineering, vol. 40, no. 8, p. 1554-1562, August 2001.

[55] I. S. Gradshteyn and I. M. Ryzhik, Table of Integrals, Series, and Products, 7th ed. New York: Academic, 2007.

[56] ANDREWS, L. C., PHILLIPS, R. L. Laser Beam Propagation through Random Media. SPIE Press, 1998.

[57] J. W. Goodman, Statistical Optics, John Wiley &Sons, 1985.

[58] P.S. Bithas, N.C. Sagias, P.T. Mathiopoulos, G.K. Karagiannidis, and A.A. Rontogiannis, "On the performance analysis of digital communications over Generalized-K fading channels," IEEE Commun. Letters, vol. 10, no. 5, pp. 353–355, May 2006.

[59] H. Willebrand and B. S. Ghuman,Free Space Optics: Enabling Optical Connectivity in Today's Networks. Indianapolis, IN: Sams Publishing, 2002.

[60] S. M. Navidpour, M. Uysal, and M. Kavehrad, “BER performance of free-space optical transmission with spatial diversity,” IEEE Trans. on Wireless Commun., vol. 6, no. 8, pp. 2813–2819, Aug. 2007.

[61] Wolfram (2014) the wolfram functions website http: // functions.wolfram.com.